A MATHEMATICAL MODEL OF HEPATITIS C VIRUS INFECTION INCORPORATING IMMUNE RESPONSES AND CELL PROLIFERATION

By

HUDA AMER HADI

THESIS

Presented to the Faculty of the Graduate School of

The University of Texas at Arlington in Partial Fulfillment

of the Requirements for the Degree of Master of Science in Mathematics

THE UNIVERSITY OF TEXAS AT ARLINGTON

August 2017

Arlington, Texas

Supervising Committee:

Hristo Kojouharov, Supervising Professor

Benito Chen Charpentier

Guojun Liao

DEDICATION I

To my husband Saleh. Thank you from now until forever for your support of my studies, your patience, and encouragement to achieve my educational goals.

April 20, 2017

DEDICATION II

This thesis is dedicated to my beloved parents. I am eternally thankful for all their love, support and encouragement. They always stood beside me in good and bad times with their unconditional love and patience. I appreciate to no end the sacrifices you made and the opportunities you afforded me to create a strong foundation upon which I have built to be where I am today.

I would like to give my greatest thanks to my husband. With you by my side, your unwavering support and endless encouragement fueled my motivation to persevere to the end. I cannot thank you enough. I strive to make you proud.

I also would like to dedicate this thesis to my brother Assel and sisters Aliaa, Rashaq, Duaa, and Nabaa. They have played such an important role throughout my life.

Finally, I dedicate this thesis to my hope and sunshine in this world, my son, little Yoseph wishing him the best future.

April 20, 2017

ACKNOWLEDGEMENTS

First and foremost, I would like to express my deepest gratitude to my advisor, Dr. Hristo Kojouharov, for his profound insight, constant guidance, support, assistance, and inspiring mentorship as both a professor in the classroom and my thesis advisor. His knowledge, experience, and unwavering encouragement proved invaluable as I progressed towards the culmination of this degree. This work would have not been possible without his supporting efforts.

I would like to thank my defense committee, Dr. Benito Chen Charpentier and Dr. Guojun Liao for the suggestions they gave during the revision process. I would also like to thank them for all the help they offered me throughout my time as a student in the math department at UTA.

I also wish to express my thanks to Dr. Jianzhong Su for his leadership in a superb mathematics department, and the remainder of the math faculty who helped shape me into the academic I am today. I am eternally grateful for the opportunities and experiences the university and department has provided me.

Finally, though too numerous for specific mentioning, I am thankful for the many teachers, instructors, and professors at the primary, secondary, and collegiate level from whom I learned valuable wisdom and a mountain of knowledge.

April 20, 2017

ABSTRACT

A MATHEMATICAL MODEL OF HEPATITIS C VIRUS INFECTION INCORPORATING IMMUNE RESPONSES AND CELL PROLIFERATION

HUDA AMER HADI, M.S.

The University of Texas at Arlington, 2017

Supervising Professor: Hristo Kojouharov

This thesis introduces a mathematical model of differential equations for the chronic hepatitis C virus (HCV) infection, which is a contagious disease that infects the liver cells. Firstly, we present the early mathematical models for the basic dynamics of virus infection that developed and analyzed to understand the dynamics of human immunodeficiency virus (HIV), hepatitis B virus (HBV), and some other viruses. Next, we present the extended model of the basic HCV virus dynamics that incorporate the effectiveness of a treatment. After that, the mathematical model that includes proliferation terms for both infected and uninfected hepatocytes is discussed. Lastly, the mathematical model that is considering the interaction between HCV virus and immune responses in a host is introduced.

In this thesis, we formulate an ordinary differential equations (ODE) model to describe the interactions between the hepatitis C (HCV) virus and the immune system in a human body under treatment, taking into consideration the proliferation for both infected and uninfected hepatocytes. Analysis of the model reveals the existence of multiple equilibrium states: the disease-free steady state in which no virus is present, an infected state with no immune

responses, an infected steady state with immune responses in which virus and infected cells are present, an infected steady state with dominant CTLs responses in which no antibody (B-cell) is present, an infected steady state with dominant antibody responses in which no CTLs is present, and an infected steady state with coexistence responses in which all are present. Finally, we run simulations and compare our model to other models in the literature. In addition, several different scenarios were numerically simulated to demonstrate the practical applications of the mathematical model.

TABLE OF CONTENTS

LIST OF TABLES

LIST OF FIGURES

ABBREVIATIONS

HCV	Hepatitis C Virus
HAV	Hepatitis A Virus
HBV	Hepatitis B Virus
HIV	Human Immunodeficiency Virus
IFN-α	Interferon- α
Peg-IFN	Pegylated Interferon
RBV	Ribavirin
DAAs	Direct-Acting Antivirals
HCV-RNA	Ribonucleic Acid of the Hepatitis C Virus
NK	Natural Killer
RNA	Registered Nurse Anesthetist
CTLs	Cytotoxic T-lymphocytes
MHC II	Major Histocompability Complex Type II
MHC I	Major Histocompability Complex Type I
ODE	Ordinary Differential Equation
ALT	Alanine Transaminase
CD4	Cluster of Differentiation 4
CD8	Cluster of Differentiation 8

CHAPTER 1

INTRODUCTION

1.1 Background Information

The liver is the biggest organ in the body, and it plays an important role in all metabolic processes in the body [19]. The main job of the liver is to filter the blood, fight infections among other functions. Once the liver is infected, its functions are affected too. Illnesses, some medications, heavy alcohol usage, and toxins can cause hepatitis. However, viruses, which are small infectious agents, are able to replicate inside the living cells of an organism; they are the most popular cause for hepatitis that is why it is often called 'viral hepatitis' [9]. There are numerous kinds of viral hepatitis such as A, B, C, D, and E. The most well-known sorts of viral hepatitis will be hepatitis A virus (HAV), hepatitis B virus (HBV), and hepatitis C virus (HCV).

Hepatitis C virus infection emerged after most blood transfusion infections were associated with either hepatitis A (HAV) or hepatitis B (HBV) virus [12]. It was first identified in 1989 when a team of Choo, Qui Lim [7] isolated this single stranded RNA from the serum of infected chimpanzees. They re-named the Non-A, Non-B hepatitis as hepatitis C.

In this thesis, we are interested in studying chronic hepatitis C virus (HCV) since it is a very dangerous disease and widely spread that may cause serious health problems, such as cirrhosis and hepatocellular carcinoma. Hepatitis C is an infectious liver disease that is caused by a small RNA virus [18]. It transmits through direct contact with the blood of an infected person with hepatitis C virus, e.g. blood transfusions and organ transplants, inadequate cleaning of medical equipment, sharing needles, or other equipment to inject drugs. Worldwide, about 185 million people are chronically infected with hepatitis C virus [24], and approximately 700,000

people die every year from hepatitis C virus in relation to liver diseases [43]. For HCV infection, the vaccine does not exist yet, but the active research is ongoing.

Hepatitis C virus infection emerged after most blood transfusion infections were associated with either hepatitis A (HAV) or hepatitis B (HBV) virus [12]. It was first identified in 1989 when a team of Choo [7] isolated this single stranded RNA from the serum of infected chimpanzees. They re-named the Non-A, Non-B hepatitis as hepatitis C.

After exposure to HCV, a strong host immune response is launched [36]. Thus, in some patients with hepatitis C virus infection will naturally clear the virus during the early phase of infection without medical intervention. They will become better on their own after several weeks to several months. However, the response fails to eradicate the virus, leading to chronic infection in which the body's immune system does not naturally clear the virus [21]. Hoofnagle (2002) [18] asserts that about 55% to 85% of HCV patients do not clear the virus themselves and develop chronic hepatitis C infection. The slow progressing liver disease is caused by a chronic HCV infection [10]. In a majority of people, the chronic HCV infection can cause severe liver problems, such as cirrhosis (scarring of the liver), liver cancer, or death [3]. Hepatitis C progresses to become chronic HCV infection due to the weak immune response against HCV [16]. When hepatitis becomes a chronic or long-period illness, the infection may need to be treated with specific medications called antivirals [39]. Antiviral therapy has been used to cure chronically HCV infected patients. It is currently the only available treatment because of the lack of an HCV vaccine [38]. Nevertheless, research to discover the HCV vaccine is outgoing. For several years, combinations of antivirals such as interferon-α (IFN- α) and ribavirin (RBV), pegylated-interferon (PEG-INF) and ribavirin (RVB) have been established as effective in viral clearance. In other words, they have been used as medication to reduce the levels of HCV-RNA.

Newly, direct-acting antivirals (DAAs) is the most common way that is used to give treatments that target particular steps of the life cycle of the HCV. However, antiviral therapy is expensive, associated with side effects, and not effective in all patients. Dahari et al., and Jirillo (2007, 2008) [8, 21] asserted that the virus is not eliminated in about 50% of patients that have a chronic HCV and that are treated with a combination treatment of Peg-IFN and RBV. [8, 21]. The goal of treatment is to cure the infection rather than suppress the virus. Additional details about these types of treatments can be found in [8, 21, 17, 26, 37].

1.2 Immune Responses

The complex system of cells, organs, proteins, and tissues that protect our body versus foreign pathogens ex. certain fungi, bacteria, germs, and viruses, is called the immune system. The immune system has been classified into two nature types of responses against foraying pathogens [42, 11]. The first nature type of response is innate or non-specific immune, and the second nature type of response is specific or adaptive immune [6]. Thus, both types, innate and adaptive immunity, are important features of the immune system and each feature varies in its response and how fast it responds. The first line of protect versus infections is the innate immune responses including sneezing, fever, and coughing. Hence, the innate immune response represents an essential character in the early recognition of foraying pathogens [27]. The innate immune system cells such as natural killer (NK) and macrophages are always ready to fight microbes and all other pathogens in a non-specific way, no matter what kind of pathogen they are fighting. However, this kind of response cannot recognize some pathogens and then eliminate infectious organisms [20]. Oppositely, the adaptive immune responses are more complex than the innate immune responses [27]. They are responsible for recognizing the physical structure of a pathogen [42]. Once an antigen has been recognized, the adaptive immune system is able to create an army of immune cells for neutralizing or eliminating the antigen. The adaptive responses can perceive proteins that are shaped from the pathogen. When the adaptive responses are activated, they begin to divide in numbers. The lymphocytes, which are white blood cells, are the most paramount factor of the adaptive immune system. They can be grouped into two important kinds of cells; B-lymphocytes, which is called B-cells, and T-lymphocytes, which is called T-cells [42, 11].

B-cells and T-cells are the fundamental players in the host immune response. B-cells produce antibodies. They are named as B-cells because they are produced in the human's bone marrow [11]. They are distinct from other cells because they have a protein (antibody) on their surface called the B-cell receptor [11]. This receptor is able to recognize and bind to specific pathogen such as bacteria and viruses interaction which makes a figure similar to a lock and key [11, 32]. It is worthy to mention that one microliter of human blood includes approximately 2500 lymphocytes, and in adult human, totally there are about 10^{12} lymphocytes [32]. The immune system is capable of making billions of different types of antibodies with a limited number of genes by rearranging DNA segments during B-cell development [37]. In fact, there is a specific antibody molecule that can recognize any pathogen that enters the body [32].

When a pathogen like HCV enters the human body, there are some specific B-cells receptors which can recognize this foreign intruder and are able to bind some viral proteins. However, some B-cells do not have the specific receptors to recognize this foreign antigen. An operation known as endocytosis starts when a B-cell is bound to the virus particle. In this operation, the virus is broken into pieces and part of it is given in association with the so-called major histocompability complex type II (MHC II), which is a molecule on the B-cell surface [42, 11, 32].

B-cells begin to divide into memory and effector cells once they are activated. These new B-cells are repetitions with the same certain receptors that can recognize HCV. The memory B-cells will stay in the system in case HCV enters the host in the future, but they take no action [11, 32]. On the other hand, the effector B-cells, which are called plasma cells, are responsible for the release of new antibodies. At that point, these antibodies bind to the infection particles and mark them as foreign pathogens for disposal by a macrophage [11].

T-cells come into two different types of cells, T-helper cells and T-killer cells (cytotoxic T-lymphocytes (CTLs)). T-helper cells are considered an essential part in the activation of the B-cells and, in this way, in the release of antibodies. On the other hand, CTLs can recognize the infected cells and then kill them. T-helper cells are also called CD4+ T cells because they release the CD4 protein on their surfaces [11]. CTLs are also called CD8+ T cells because they release the CD8 glycoprotein at their surfaces [11]**.** When a cell has been infected, it produces a new virus. Inside the infected cell the viral proteins are introduced on the surface in a blend with the major histocompability complex type I (MHC I), which is introduced basically in each cell of the human body. The T-cell receptor with specific CTL is able to recognize these introduced proteins on the infected cells surface and then it will link to the cell. After that, the CTLs will split into memory and effector cells. The job of memory cells is to remain in the host in case of new infection occurring in the future. On the other hand, the job of effector cells is to eliminate infected cells. The two types of immune system responses are shown in Figure 1. The explanation of the process of the immune system responses are shown in Figure 2.

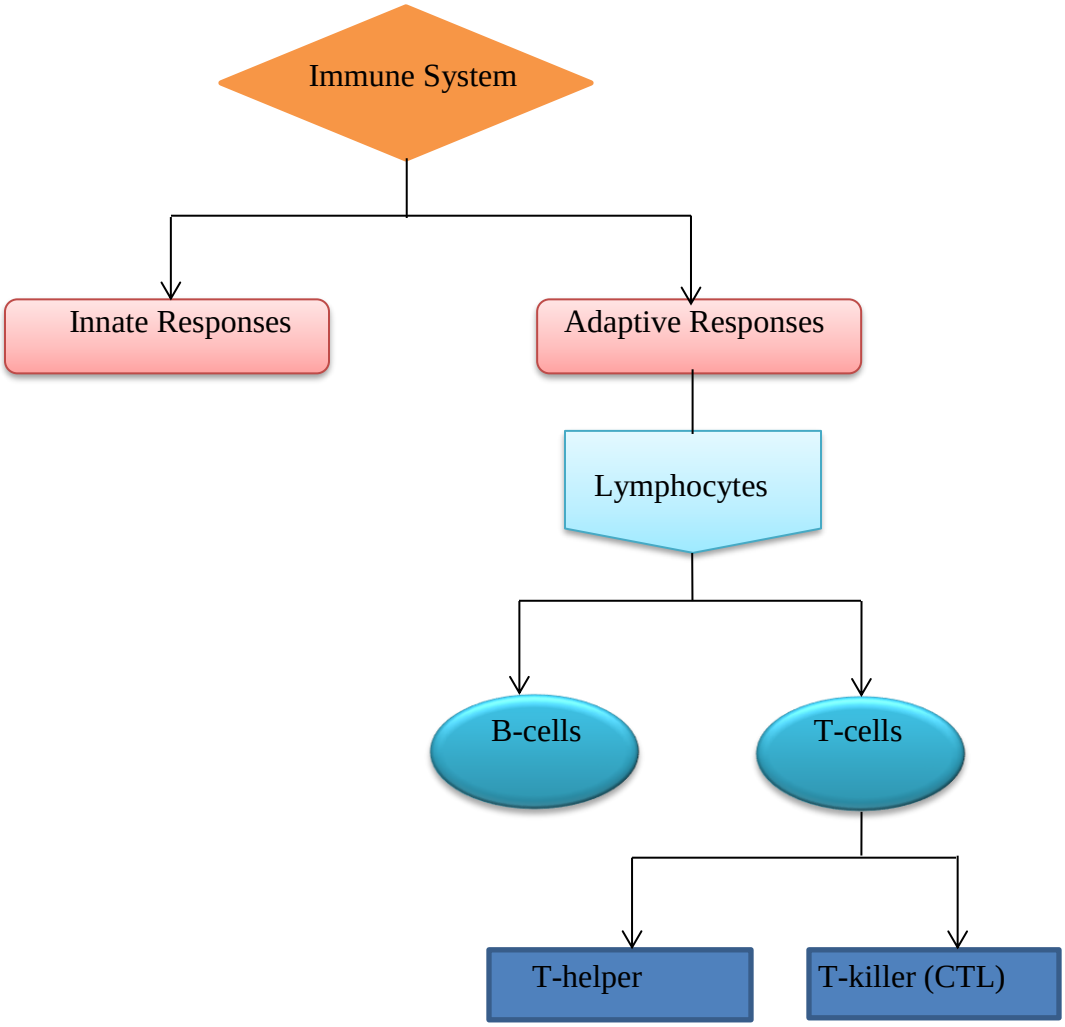

Figure 1: A schematic illustration of the two different kinds of immune system responses: the adaptive and the innate responses. The most paramount factor of the adaptive responses is the lymphocytes that can be grouped into B-cells and T-cells.

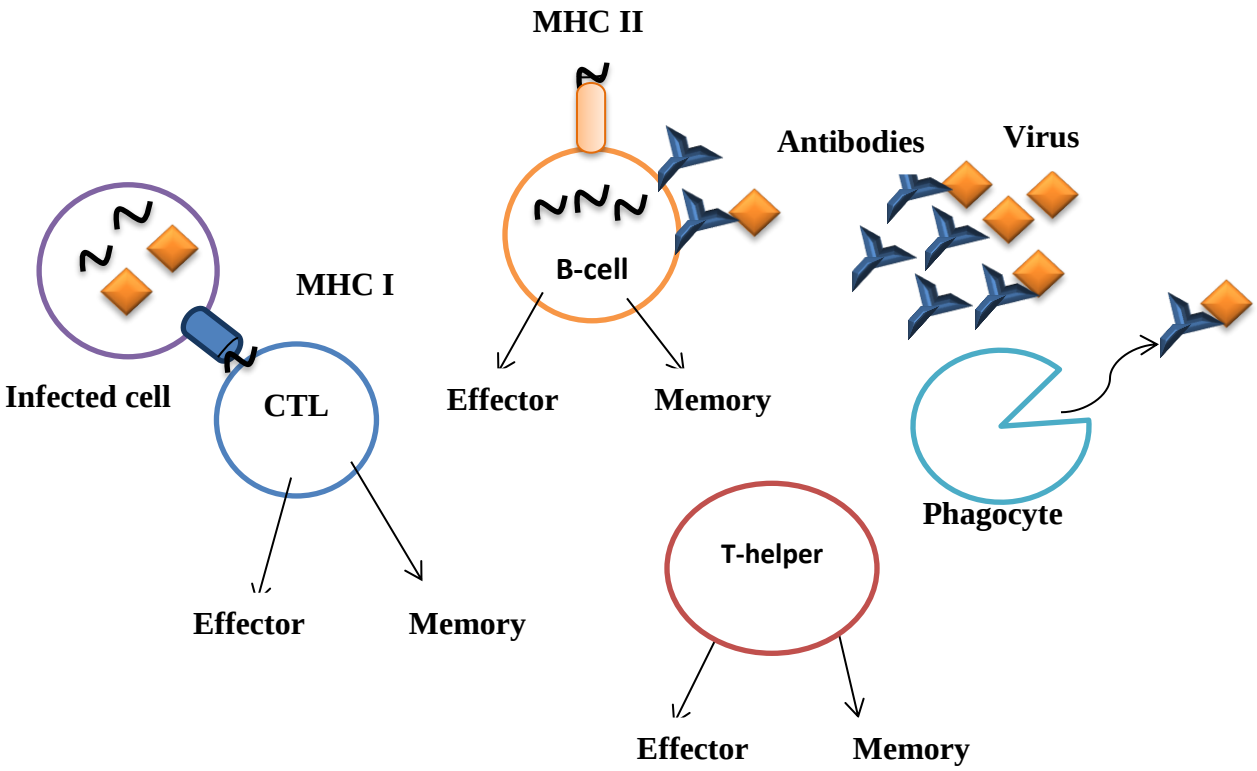

Figure 2: A schematic illustration of the adaptive responses. The adaptive responses can be classified into B-cells and T-cells. The job of B-cells is producing antibodies that can help to neutralize virus particles. CTLs eliminate infected cells. Phagocytes are immune cells group can find and eat virus particles that have been controlled by antibodies.

The interactions between pathogens and immune responses can be viewed as a predator-prey system. The predator is the immune cells like the B-cells and T-cells and the prey is the virus. The predator types can minimize the sustenance resource to levels that are too low for other predator types to survive. In other words, antibodies can reduce the virus load to very low levels to activate the CTLs when they are more efficient in capturing the virus. This result will be called the dominant responses of antibodies. Similarly, CTLs can reduce the virus load to very low levels to activate the antibodies when they are more efficient in killing the pathogen. This result will be called the dominant responses of CTLs. Further details about the immune responses can be found in [11, 32].

CHAPTER 2

A REVIEW OF THE RELEVANT LITERATURE

In this section, we first consider the early basic ordinary differential equation (ODE) model that has been applied to virus dynamics in-vivo. Then, we show the original mathematical model of viral dynamics in-vivo under antiviral therapy. This model had proved very successful in understanding the pathogenesis and guiding therapy for hepatitis C virus (HCV) infection. After that, we introduce the extended model of the original model that considers the proliferation of liver cells. Finally, we proceed to introduce the model that shows the interaction between the immune response and hepatitis C virus (HCV).

Mathematical modeling is a useful tool in the study of virus dynamics because it helps to understand the biological mechanisms involved and interpret the experimental results. The early mathematical model for the basic dynamics of virus in-vivo was developed and analyzed in [2, 31, 33, 35] to understand the dynamics of HIV, hepatitis B (HBV) and some other viruses infection. The basic principles of the early virus dynamics model in-vivo are shown in Figure 3. The model design is based on three variables: the number of uninfected or target cells, T, that infected when they meet free viruses, V, the number of infected cells, I, that produce new virus particles that leave the cell and find other uninfected cells.

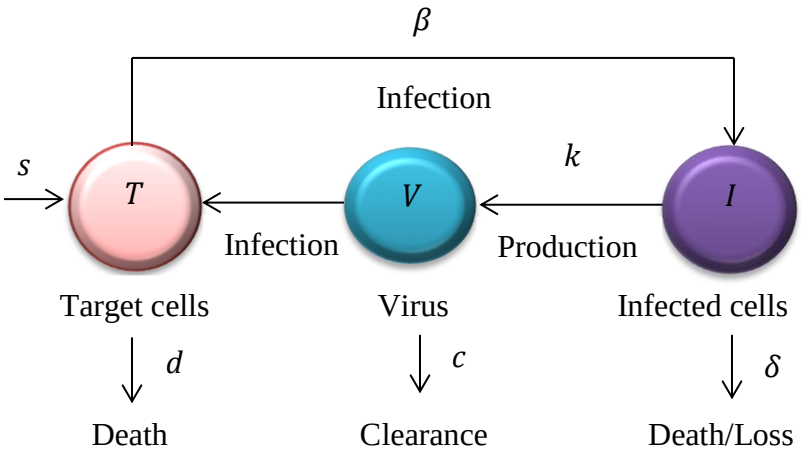

Figure 3: A schematic diagram of the basic model of viral infection.

The basic model of virus dynamics can be written in the chemical reaction notation

$$T + V \rightarrow I \rightarrow kV$$

The uninfected cells, T, over its lifespan is assumed to produce viral particles, k [25]. The equations that describe the interaction between these cells and virus particles are given by ordinary differential equations (1):

$$\begin{aligned} \frac{dT}{dt} &= s - dT - \beta VT \\ \frac{dI}{dt} &= \beta VT \\ &\quad - \delta I \\ \frac{dV}{dt} &= kI - cV \end{aligned} \tag{1}$$

This model assumes that uninfected cells, T, are produced at a rate, s, and they are subject to natural death at a rate, dT, and become infected by the interaction with virus at a rate, βVT. Infected cells, I , are naturally die at a rate, δI. Free virus is produced by infected cells at a rate, kI, and clearance at a rate, cV. Thus, the average lifetime of an infected cell is $\frac{1}{\delta}$; the average

lifetime of a free virus particle is $\frac{1}{c}$; the total number of virus particles produced from one infected cell is $\frac{k}{\delta}$.

After the discovery of hepatitis virus type C, it became significant to study the dynamics of the virus in-vivo. In literature, various models have been utilized to depict hepatitis C virus (HCV) dynamics [8, 29, 41]. Thus, with a chronic hepatitis C virus (HCV), it was necessary to understand the dynamics of the virus in-vivo and to determine the need for treatment for a disease with such a long progression term. For several years, antiviral therapy has been used as a treatment to reduce the levels of HCV- RNA. Around then, mathematical modeling of virus dynamics in-vivo under treatment assumed an extremely valuable part to comprehend the pathogenesis and controlling treatment of chronic HCV. Perelson et al., 2005 [34] said that the modeling of the virus kinetics has assumed a critical part in the analysis of HCV-RNA decay through antiviral therapy. The first mathematical model, which is inspired from (1), is utilized to examine the dynamic of chronic HCV- RNA and the antiviral impact of interferon alfa (IFN-α) in 1996 [45]. The authors in [45] considered two ordinary differential equations; one for the infected hepatocytes, and the other one for the free virus. They observed that the IFN-α treatment can be blocking new infection with 100% efficacy or blocking viral production with 100% efficacy, and most patients showed a biphasic viral decline [45, 46].

Neumann et al., (1998) [29] extended the previous model in [45] by including a separate differential equation for healthy hepatocytes. This model, which is called original model, also describes the viral kinetics in HCV patients during IFN-α treatment (Figure 4).

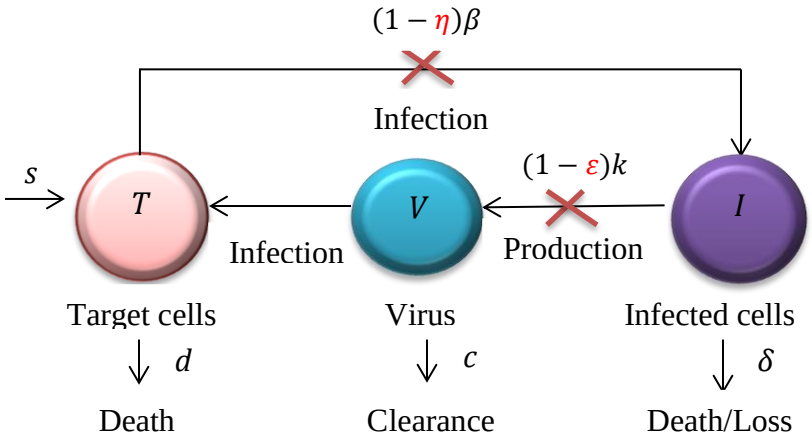

Figure 4: A schematic diagram of the original viral kinetic model under treatment.

Treatment is assumed to act by blocking new infection with an effectiveness, η, or by blocking virus production with an effectiveness, ε. The remaining parameters are defined similarly to the model (1).

The original model during treatment is given by the following system of ordinary differential equations (2):

$$\frac{dT}{dt} = s - dT - (1-\eta)\beta VT$$

$$\frac{dI}{dt} = (1-\eta)\beta VT - \delta I \qquad (2)$$

$$\frac{dV}{dt} = (1-\varepsilon)kI - cV$$

This model assumes that the possible effects of IFN-α in this model act by blocking either the production of virus from infected cells through fraction $(1-\varepsilon)$, or the new infection by fraction $(1-\eta)$. In other words, ε is the efficacy of the drug in blocking production of the virus from infected cells and η is the efficacy of the drug in stopping infection. The remaining parameters are defined similarly to the basic model (1). The authors observed that daily IFN-α doses of 5, 10, and 15 mIU on 23 patients were correlated to release the viral and production blocking efficacy of 81, 95 and 96% efficacy respectively. Moreover, they asserted that the half-life of the virus ($t_{1/2}$) was on average 2.7 hours, and eliminate 10^{12} viruses per day. Also, they said that the expected death rate of the infected cell showed a big interpatient difference (comparing $t_{1/2}$= 1.7 to 70 days). It was inversely with baseline virus load, and was positively with alanine aminotransferase levels (ALT), which is an enzyme that spilled into the blood stream when the liver is injured [29]. They concluded that it is important to control the dynamic of HCV virus in the early phase of their stage to help to guide treatment because it has a very high dynamic. After that, several articles were published to use this model to better understand HCV infection.

As mentioned before, the original model (2) of chronic HCV infection under treatment that has been proposed by Neumann et al. (1998), which expects a constant population of healthy cells with a rate, s, was applied to estimate the rates of virus clearance and infected cell death.

The decay of HCV-RNA noticed in patients in the first 14 days of treatment [29]. However, this original model is definitely not ready to explain some watched HCV-RNA dynamic profiles under therapy [8].

The liver is an organ that is regenerate because of the homeostatic system in-vivo [15, 28]. Thus, any loss in the hepatocytes can be compensated by the proliferation of the existing hepatocytes [15, 28]. The previous model (2) ignores the proliferation of both infected I and uninfected T cells [8]. Therefore, Dahari et al. (2007) [8] extended the original model (2) by adding a proliferation terms r for both infected and uninfected hepatocytes (Figure 5) that allow the total number $(T + I)$ of liver cells to reach a maximum size, T_{max}.

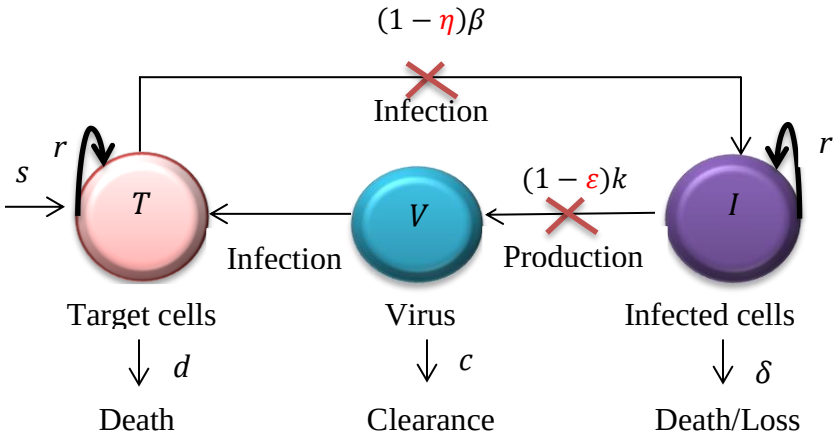

Figure 5: A schematic diagram that illustrates the extended model accounting for hepatocyte proliferation. Both uninfected and infected liver cells proliferate logistically with maximum rate, r, until the total number of hepatocytes reachesT_{max}.

The corresponding differential equations of the extended mathematical model (2) are given by:

$$\frac{dT}{dt} = s + rT\left(1 - \frac{T+I}{T_{max}}\right) - dT - (1-\eta)\beta VT$$

$$\frac{dI}{dt} = (1-\eta)\beta VT + rI\left(1 - \frac{T+I}{T_{max}}\right) - \delta I \qquad (3)$$

$$\frac{dV}{dt} = (1-\varepsilon)kI - cV$$

In this model, r represents the maximum proliferation rate of the uninfected, T, and infected, I, hepatocytes, which means that T and I hepatocytes can proliferate under a blind homeostasis process, in which there is no distinction between infected and uninfected cells in the density-dependent term. Dahari et al. (2007) [8] confirmed that the maximum rate of the spread of r, can be different for the infected and uninfected cells, and will continue this circular life anywhere else. The number $(T + I)$ represents the total hepatocyte population which can increase up to a maximum of T_{max}. The remaining parameters are defined similarly to the original model (2). The presentation of the hepatocytes proliferation in this model (3) is the new advantage that has demonstrated an important role in understanding the viral dynamics later on. Also, their views are very essential in the results of my thesis.

It is worth to mention that the previous mathematical models ignore the responses of the immune system which is considered the most important factor in stimulating therapeutic cells. The immune system interacts against viruses through viral infection [14]. Nowak and Bangham (1996) [31] emphasize that immune responses have a significant role to reduce the virus load. Miao et al. (2016) [14] said that the CTL and the antibody both have the ability in prohibition and controlling infections. The immune response of the CTL is responsible to ban the reproduction of the virus, and the immune response of the antibody is responsible to neutralize the virus in-vivo [14]. Therefore, Wodarz (2003) [41] proposed a model that deals with the interaction between HCV and immune responses in a host. This model extended to model (1), given by adding two differential equations, one represents the number of CTLs and is denoted by Z, and the other one represents the number of the antibody response and is denoted by W. Figure 6 illustrates the immune system responses.

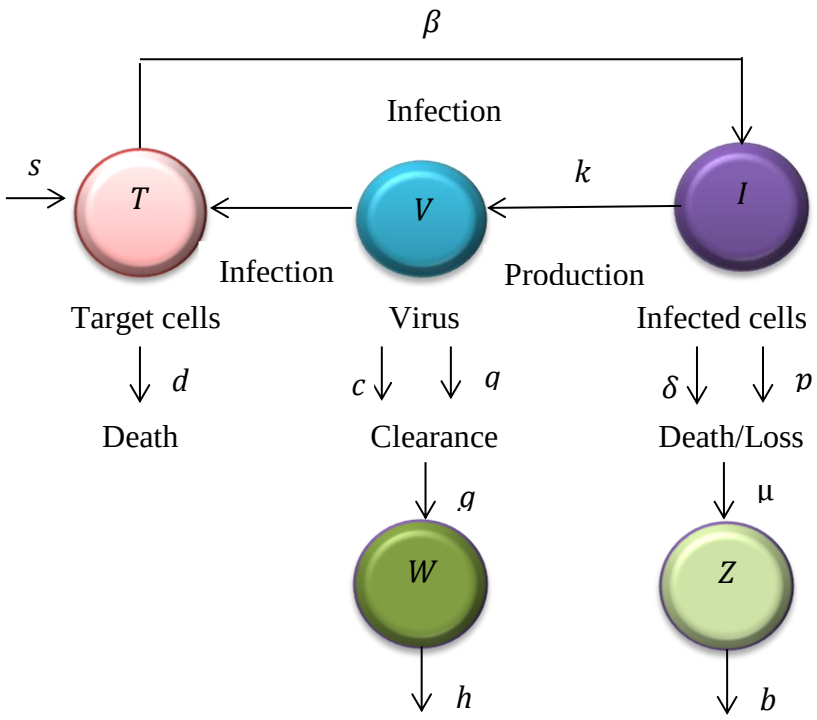

Figure 6: A schematic diagram that illustrates the immune system responses.

Consider the extension of (1) given by the system of ordinary differential equations (4)

$$\frac{dT}{dt} = s - dT - \beta VT$$

$$\frac{dI}{dt} = \beta VT - \delta I - pIZ$$

$$\frac{dV}{dt} = kI - cV - qVW \qquad (4)$$

$$\frac{dZ}{dt} = \mu IZ - bZ$$

$$\frac{dW}{dt} = gVW - hW$$

Here, pIZ represents the rate of killing the infected cells by the CTL response, and the qVW represents the rate of neutralized virus particles by the antibody. In response to virus antigen that is produced from infected cells, I, at a rate μIZ, CTLs increase. Also, CTLs decay at

rate bZ in the lack of antigenic stimulation. In response to virus particles, antibodies progress at a rate gVW. In addition, antibody decay at a rate hW. Properties of the solutions such as positivity, boundedness, non-periodicity, and limiting behavior, as well as the stability analysis of the model were discussed in [44]. The model in [41] showed that the infected cells can be controlled by the antibody responses and the persistent infection can activate the antibody responses while the levels of the CTLs responses are not preserved at high levels. However, the result of facing the persistent infection can change the immune responses' balance and lead to increase the weak CTLs levels more than the antibody responses [41]. This change can cause to develop the virus and it is led to chronic liver pathology [41]. Thus, it was concluded that the immune response balance plays a crucial role in controlling the virus as it develops over time. However, the role of the antibody and CTLs is not completely understood yet [14, 23].

CHAPTER 3

The New Mathematical Model of Hepatitis C Virus Infection

3.1 Mathematical Model Description

In this thesis we are interested in understanding the interactions between the hepatitis C virus and the immune system under treatment, taking into consideration the proliferation for both infected and uninfected hepatocytes.

The aim is to combine model (3) and model (4) to obtain a new mathematical model of HCV that incorporates the immune system and cell proliferation. Figure 7 is a depiction of this model.

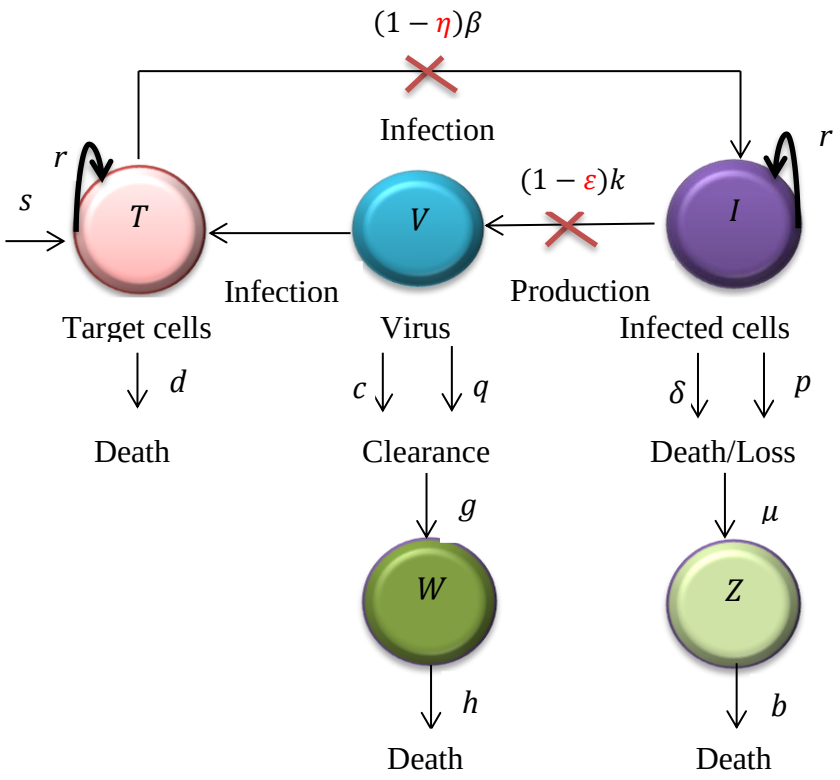

Figure 7: A schematic diagram that illustrates a combination of model (3) and model (4).

The new mathematical model is as follows:

$$\frac{dT}{dt} = s + rT\left(1 - \frac{T+I}{T_{max}}\right) - dT - (1-\eta)\beta VT$$

$$\frac{dI}{dt} = (1-\eta)\beta VT + rI(1 - \frac{T+I}{T_{max}}) - \delta I - pIZ \qquad (5)$$

$$\frac{dV}{dt} = (1-\varepsilon)kI - cV - qVW$$

$$\frac{dZ}{dt} = \mu IZ - bZ$$

$$\frac{dW}{dt} = gVW - hW$$

The parameters that are used in the model (5) are defined similarly to models (3) and (4) and listed with their units in Table 1.

Table 1: The interpretation of the parameters used in model (5) and their units.

Parameters	Interpretation	Units
T_{max}	maximum size of growth of the liver	cells ml^{-1}
s	natural production rate of healthy cells (T)	cells $ml^{-1}day^{-1}$
r	the maximum proliferation rate of the uninfected (T) and infected (I) cells	day^{-1}

d	natural death rate of healthy cells (T)	day^{-1}
β	the rate at which virus (V) infects healthy cells (T)	ml day^{-1} $virions^{-1}$
δ	natural death rate of infected cells (I)	day^{-1}
p	the rate at which CTLs (Z) kills infected cells (I)	day^{-1}
k	production rate of the virus particles (V) from infected cells (I)	virions $cells^{-1}$ day^{-1}
c	natural clearance rate of virus particles (V)	day^{-1}
q	the rate at which antibody (W) neutralized the virus particles (V)	day^{-1}
μ	expand rate of CTLs (Z) in response to virus antigen derived from infected cells (I)	day^{-1}
b	natural decay rate of CTLs (Z) in the absence of antigenic stimulation	day_{-1}
g	development rate of antibody (W) in response to virus particles (V)	day^{-1}
h	natural decay rate of antibody (W)	day^{-1}
ε	the efficacy of the drug in blocking virus production from infected cells (I)	unit less
η	the efficacy of the drug in stopping new infection	unit less

3.2 Equilibria and their Stability

3.2.1 Equilibrium solutions

To determine the stability of the above model (5), we evaluate the equilibrium points or steady states of this model. Equilibrium points of model (5) can be found by setting the right-hand side of the equations to zero and then solve for the values of T, I, V, Z, and W.

At the steady state,

$$\frac{dT}{dt} = 0, \frac{dI}{dt} = 0, \frac{dV}{dt} = 0, \frac{dZ}{dt} = 0, and\ \frac{dW}{dt} = 0$$

where

$$s + rT\left(1 - \frac{T+I}{T_{max}}\right) - dT - (1-\eta)\beta VT = 0 \qquad (3.1)$$

$$(1-\eta)\beta VT + r\,I\left(1 - \frac{T+I}{T_{max}}\right) - \delta I - pIZ = 0 \qquad (3.2)$$

$$(1-\varepsilon)kI - cV - qVW = 0 \qquad (3.3)$$

$$\mu IZ - bZ = 0 \qquad (3.4)$$

$$gVW - hW = 0 \qquad (3.5)$$

Like other mathematical models, this model has an equilibrium point called disease-free equilibrium. This represents the absence of virus (i.e., $V_0^* = 0$). After solving Equations (3.1) - (3.5), we obtain the uninfected equilibrium state which is given by:

$$(T_0^*, I_0^*, V_0^*, Z_0^*, W_0^*) = (\frac{T_{max}}{2r}\left[r - d + \sqrt{(r-d)^2 + \frac{4rs}{T_{max}}}\right], 0,0,0,0),$$

where $r > d$ and $s \leq dT_{max}$ with a specific aim to have a physiologically factual model (i.e., $T0 \leq T_{max}$). The same result is found in [8], in which there is no infection. Thus, all hepatic cells are uninfected (healthy) and $T_0^* = \frac{T_{max}}{2r}\left[r - d + \sqrt{(r-d)^2 + \frac{4rs}{T_{max}}}\right]$ is the number of liver cells in one healthy individual.

If $V_1^* \neq 0$, then the following infected equilibrium point solution is found by solving equations (3.4) and (3.5) in model (5) to obtain $Z_1^* = W_1^* = 0$, which represents the absence of immune responses. As a result, model (5) converges to the second equilibrium point given by:

$$(T_1^*, I_1^*, V_1^*, Z_1^*, W_1^*) = (\frac{1}{2}\left[-D + \sqrt{D^2 + \frac{4sT_{max}}{rA^2}}\right], T_1^*(A-1) + T_{max} - B, \frac{(1-\varepsilon)kI_1^*}{c}, 0,0),$$

where

$$A = \frac{(1-\eta)(1-\varepsilon)k\beta T_{max}}{cr},$$

$$B = \frac{\delta T_{max}}{r},$$

$$D = \frac{1}{A}\left(T_{max} + \frac{dB}{\delta A} - B\left(\frac{1}{A} + 1\right)\right).$$

This is called an infected equilibrium state with no immune responses; the same result is also shown in [8].

Dominant CTLs response is the third infected equilibrium state observed. This represents the absence of antibody response (i.e., $W_2^* = 0$).

Solving equation (3.4) to obtain

$$I_2^* = \frac{b}{\mu}, \tag{3.6}$$

and equation (3.5) to obtain

$$W_2^* = 0, \tag{3.7}$$

Then, substitute equations (3.6) and (3.7) in equation (3.3) to attain

$$V_2^* = \frac{(1-\varepsilon)kb}{\mu c}, \tag{3.8}$$

Then, from (3.1) we achieve

$$s + rT - \frac{rT^2 + rTI_2^*}{T_{max}} - dT - (1-\eta)\beta V_2^* T = 0,$$

$$\Rightarrow \quad \left(-\frac{r}{T_{max}}\right)T^2 + \left(r - \frac{rI_2^*}{T_{max}} - d - (1-\eta)\beta V_2^*\right)T + s = 0,$$

After that, using the quadratic formula to obtain T_2^* as following:

$$T_2^* = \frac{-\left(r - \frac{rI_2^*}{T_{max}} - d - (1-\eta)\beta V_2^*\right) \pm \sqrt{\left(r - \frac{rI_2^*}{T_{max}} - d - (1-\eta)\beta V_2^*\right)^2 - 4\left(-\frac{r}{T_{max}}\right)s}}{2\left(-\frac{r}{T_{max}}\right)}, \tag{3.9}$$

$$\Rightarrow \qquad T_2^* = \frac{T_{max}}{2r}\left(r - d - \frac{rb}{\mu T_{max}} - \frac{(1-\eta)(1-\varepsilon)kb\beta}{\mu c} \pm \sqrt{\left(r - d - \frac{rb}{\mu T_{max}} - \frac{(1-\eta)(1-\varepsilon)kb\beta}{\mu c}\right)^2 + \frac{4rs}{T_{max}}}\right),$$

$$\therefore\ T_2^* = \frac{T_{max}}{2r}\left(F + \sqrt{F^2 + Q}\right). \tag{3.10}$$

where

$F = r - d - \frac{rb}{\mu T_{max}} - \frac{(1-\eta)(1-\varepsilon)kb\beta}{\mu c}$ and $Q = \frac{4rs}{T_{max}}$.

Then, substitute equations (3.6), (3.8), and (3.10) in equation (3.2) to attain

$$\therefore Z_2^* = \frac{(1-\eta)\beta V_2^* T_2^* + r\, I_2^*\left(1 - \frac{T_2^* + I_2^*}{T_{max}}\right) - \delta I_2^*}{pI_2^*}\ . \tag{3.11}$$

As a result, model (5) converges to the third equilibrium point given by:

$$(T_2^*, I_2^*, V_2^*, Z_2^*, W_2^*) = \left(\frac{T_{max}}{2r}\left(F + \sqrt{F^2 + Q}\right), \frac{b}{\mu}, \frac{(1-\varepsilon)kb}{\mu c}, \frac{(1-\eta)\beta V_2^* T_2^* + r\, I_2^*\left(1 - \frac{T_2^* + I_2^*}{T_{max}}\right) - \delta I_2^*}{pI_2^*}, 0\right).$$

Dominant antibody response is the fourth infected equilibrium state observed. This represents the absence of CTLs response (i.e., $Z_3^* = 0$).

Solving equation (3.4) to obtain

$$Z_3^* = 0, \tag{3.12}$$

and equation (3.5) to obtain

$$V_3^* = \frac{h}{g}\,, \tag{3.13}$$

Then, substitute equation (3.13) in equation (3.3) to find

$$(1-\varepsilon)kI_3^* = \frac{ch + qhW_3^*}{g},$$

$$\Rightarrow \quad I_3^* = \frac{ch+qhW_3^*}{(1-\varepsilon)kg}. \tag{3.14}$$

Also, substitute equations (3.13) and (3.14) in equation (3.3) to obtain

$$W_3^* = \frac{(1-\varepsilon)kI_3^* - cV_3^*}{qV_3^*}. \tag{3.15}$$

Then, by using equation (3.9) we achieve

$$T_3^* = \frac{T_{max}}{2r}\left(r - d - \frac{rI_3^*}{T_{max}} - (1-\eta)(1-\varepsilon)\beta V_3^* \right.$$
$$\left. \pm \sqrt{\left(r - d - \frac{rI_3^*}{T_{max}} - (1-\eta)(1-\varepsilon)\beta V_3^*\right)^2 + \frac{4rs}{T_{max}}}\right), \tag{3.16}$$

$$\therefore \quad T_3^* = \frac{T_{max}}{2r}\left(U + \sqrt{U^2 + N}\right). \tag{3.17}$$

where

$U = r - d - \frac{rI_3^*}{T_{max}} - (1-\eta)(1-\varepsilon)\beta V_3^*$ and $N = \frac{4rs}{T_{max}}$.

This model (5) converges to the fourth equilibrium point given by:

$$(T_3^*, I_3^*, V_3^*, Z_3^*, W_3^*) = \left(\frac{T_{max}}{2r}\left(U + \sqrt{U^2 + N}\right), \frac{h}{g}, \frac{ch+qhW_3^*}{(1-\varepsilon)kg}, 0, \frac{(1-\varepsilon)kI_3^* - cV_3^*}{qV_3^*}\right).$$

Coexistence is the fifth equilibrium state observed.

Solving equation (3.4) to obtain

$$Z_4^* = 0, \tag{3.18}$$

and $$I_4^* = \frac{b}{\mu}, \tag{3.19}$$

Also, solving equation (3.5) to find

$$W_4^* = 0\,, \tag{3.20}$$

and $$V_4^* = \frac{h}{g}\,, \tag{3.21}$$

Then, by solving equation (3.3), we attain

$$(1-\varepsilon)kI_4^* - cV_4^* - qV_4^*W_4^* = 0,$$

$$\Rightarrow \quad (1-\varepsilon)kI_4^* = (c + qW_4^*)V_4^*\,,$$

$$\Rightarrow \quad \frac{kI_4^*}{V_4^*} = \frac{c+qW_4^*}{1-\varepsilon},$$

$$\Rightarrow \quad \frac{kI_4^*(1-\varepsilon)}{V_4^*} = c + qW_4^*,$$

$$\Rightarrow \quad qW_4^* = \frac{kI_4^*(1-\varepsilon)}{V_4^*} - c,$$

$$\Rightarrow \quad W_4^* = \frac{kI_4^*(1-\varepsilon) - V_4^*c}{V_4^*q}. \tag{3.22}$$

After that, substitute equation (3.19) and (3.21) in equation (3.22) to achieve

$$W_4^* = \frac{k\left(\frac{b}{\mu}\right)(1-\varepsilon)-\frac{h}{g}c}{\frac{h}{g}q},$$

$$\Rightarrow \quad W_4^* = \frac{gk\left(\frac{b}{\mu}\right)(1-\varepsilon)-hc}{hq},$$

$$\therefore \quad W_4^* = \frac{gkb(1-\varepsilon)-hc\mu}{hq\mu}. \qquad (3.23)$$

Now to find T_2^* and Z_2^*, we substitute equation (3.19) and (3.21) in equation (3.9) to obtain

$$T_4^* = \frac{T_{max}}{2r}\left(r - d - \frac{rI_4^*}{T_{max}} - (1-\eta)(1-\varepsilon)\beta V_4^* \right.$$

$$\left. \pm \sqrt{\left(r - d - \frac{rI_4^*}{T_{max}} - (1-\eta)(1-\varepsilon)\beta V_4^* \right)^2 + \frac{4rs}{T_{max}}} \right),$$

$$\therefore \quad T_4^* = \frac{T_{max}}{2r}\left(M + \sqrt{M^2 + H} \right). \qquad (3.24)$$

where

$M = r - d - \frac{rb}{\mu T_{max}} - \frac{(1-\eta)\beta h}{g}$, $H = \frac{4rs}{T_{max}}$.

Then, substitute equations (3.19), (3.21), and (3.24) in equation (3.2) to solve

$$\therefore \quad Z_4^* = \frac{(1-\eta)\beta V_4^* T_4^* + r\, I_4^*\left(1 - \frac{T_4^* + I_4^*}{T_{max}}\right) - \delta I_4^*}{pI_4^*} \ . \qquad (3.25)$$

This model (5) converges to the fifth equilibrium point given by:

$$(T_4^*, I_4^*, V_4^*, Z_4^*, W_4^*) = (\frac{T_{max}}{2r}\left(M + \sqrt{M^2 + H}\right), \frac{b}{\mu}, \frac{h}{g}, \frac{(1-\eta)\beta V_4^* T_4^* + r\, I_4^*\left(1 - \frac{T_4^* + I_4^*}{T_{max}}\right) - \delta I_4^*}{p I_4^*}, \frac{gkb(1-\varepsilon) - hc\mu}{hq\mu}).$$

By using Mathematica for solving model (5), we observed that this system has ten more equilibrium points that are too complicated to write all of them in this paper.

3.2.2 Stability Analysis

The local stability of the equilibrium points can be determined by linearising the non-linear equations of the mathematical model around each equilibrium point, and examining the corresponding eigenvalues of the characteristic equations [8]. By linearising the non-linear equations of model (5), the Jacobian matrix $J(T, I, V, Z, W)$ of this model is given by:

$$J(T, I, V, Z, W) =$$

$$\begin{bmatrix} r\left(1 - \frac{I+2T}{T_{max}}\right) - d - (1-\eta)\beta V & \frac{-rT}{T_{max}} & -(1-\eta)\beta T & 0 & 0 \\ (1-\eta)\beta V - \frac{rI}{T_{max}} & r\left(1 - \frac{2I+T}{T_{max}}\right) - \delta - pZ & (1-\eta)\beta T & -pI & 0 \\ 0 & (1-\varepsilon)k & -c - qW & 0 & -qV \\ 0 & \mu Z & 0 & \mu I - b & 0 \\ 0 & 0 & gW & 0 & gV - h \end{bmatrix}.$$

3.2.2.1 Stability of the Disease-Free Equilibrium

In this section, we study the stability properties of the disease-free equilibrium (uninfected steady state). First, the local stability of the disease-free equilibrium (uninfected

steady state), $(T_0^*, I_0^*, V_0^*, Z_0^*, W_0^*) = (\frac{T_{max}}{2r}\left[r - d + \sqrt{(r-d)^2 + \frac{4rs}{T_{max}}}\right], 0,0,0,0)$ is ruled by the eigenvalues of the Jacobian matrix J_0 as follows:

$$J_0(T_0^*, 0,0,0,0) = \begin{bmatrix} r\left(1 - \frac{2T_0^*}{T_{max}}\right) - d & \frac{-rT_0^*}{T_{max}} & -(1-\eta)\beta T_0^* & 0 & 0 \\ 0 & r\left(1 - \frac{T_0^*}{T_{max}}\right) - \delta & (1-\eta)\beta T_0^* & 0 & 0 \\ 0 & (1-\varepsilon)k & -c & 0 & 0 \\ 0 & 0 & 0 & -b & 0 \\ 0 & 0 & 0 & 0 & -h \end{bmatrix},$$

$$= \begin{bmatrix} r\left(1 - \frac{2T_0^*}{T_{max}}\right) - d - \lambda & \frac{-rT_0^*}{T_{max}} & -(1-\eta)\beta T_0^* & 0 & 0 \\ 0 & r\left(1 - \frac{T_0^*}{T_{max}}\right) - \delta - \lambda & (1-\eta)\beta T_0^* & 0 & 0 \\ 0 & (1-\varepsilon)k & -c - \lambda & 0 & 0 \\ 0 & 0 & 0 & -b - \lambda & 0 \\ 0 & 0 & 0 & 0 & -h - \lambda \end{bmatrix},$$

which gives $\lambda_1 = -\sqrt{(r-d)^2 + \frac{4rs}{T_{max}}}$, $\lambda_2 = -b$, and $\lambda_3 = -h$ and the other two eigenvalues are solutions of the following characteristic polynomial of the next J_0^* matrix:

$$J_0^* = \begin{bmatrix} r - \frac{rT_0^*}{T_{max}} - \delta & (1-\eta)\beta T_0^* \\ (1-\varepsilon)k & -c \end{bmatrix}.$$

The characteristic polynomial of the system is given by the following equation:

$$P_2(\lambda) = \lambda^2 - (a_{11} + a_{22})\lambda + (a_{11}a_{22} - a_{12}a_{21})$$

$$= \lambda^2 - Tr(J_0^*)\lambda + \det(J_0^*),$$

$$P_2(\lambda) = \lambda^2 - \left(r - \frac{rT_0^*}{T_{max}} - \delta - c\right)\lambda - c\left(r - \frac{rT_0^*}{T_{max}} - \delta\right) - (1-\varepsilon)(1-\eta)k\beta T_0^* \qquad (3.2.2.1)$$

$$P_2(\lambda) = \lambda^2 + a_1\lambda + a_2$$

with coefficients given by:

$$a_1 = -\left(r - \frac{rT_0^*}{T_{max}} - \delta - c\right),$$

$$a_2 = -c\left(r - \frac{rT_0^*}{T_{max}} - \delta\right) - (1-\varepsilon)(1-\eta)k\beta T_0^*.$$

If a_1 and a_2 are both positive, then the eigenvalues have negative real part (by the Routh-Hurwitz criterion) [1], which implies the asymptotic stability of this equilibrium.

1) $a_1 > 0, \quad -\left(r - \frac{rT_0^*}{T_{max}} - \delta - c\right) > 0$

This condition is satisfied if and only if

$$r - \frac{rT_0^*}{T_{max}} - \delta < -c$$

$$\Rightarrow \quad r - \frac{rT_0^*}{T_{max}} + c < \delta$$

$$\Rightarrow \quad \frac{1}{\delta}\left(r\left(1 - \frac{T_0^*}{T_{max}}\right) + c\right) < 1.$$

2) $a_2 > 0, \quad -c\left(r - \frac{rT_0^*}{T_{max}} - \delta\right) - (1-\varepsilon)(1-\eta)k\beta T_0^* > 0$

This condition is satisfied if and only if

$$-c\left(r - \frac{rT_0^*}{T_{max}} - \delta\right) - (1-\varepsilon)(1-\eta)k\beta T_0^* > 0,$$

$$\Rightarrow \quad r\left(1-\frac{T_0^*}{T_{max}}\right)-\delta<-\frac{(1-\eta)(1-\varepsilon)\beta k T_0^*}{c},$$

$$\Rightarrow \quad \frac{1}{\delta}\left(r\left(1-\frac{T_0^*}{T_{max}}\right)+\frac{(1-\eta)(1-\varepsilon)\beta k T_0^*}{c}\right)<1.$$

Accordingly for stability, this happens if and only if the coefficients of (3.2.2.1) are positive, which hold true as long as the stability condition follows:

$$-c\left(r-\frac{rT_0^*}{T_{max}}-\delta\right)-(1-\varepsilon)(1-\eta)k\beta T_0^*>0,$$

$$\Rightarrow \quad r\left(1-\frac{T_0^*}{T_{max}}\right)-\delta<-\frac{(1-\eta)(1-\varepsilon)\beta k T_0^*}{c},$$

$$\Rightarrow \quad \frac{1}{\delta}\left(r\left(1-\frac{T_0^*}{T_{max}}\right)+\frac{(1-\eta)(1-\varepsilon)\beta k T_0^*}{c}\right)<1. \qquad (3.2.2.2)$$

The equilibrium of a model is considered asymptotically stable if all the eigenvalues of the Jacobian have negative real part [4]. Therefore, the disease-free equilibrium $(T_0^*, I_0^*, V_0^*, Z_0^*, W_0^*) = (\frac{T_{max}}{2r}\left[r-d+\sqrt{(r-d)^2+\frac{4rs}{T_{max}}}\right], 0,0,0,0)$ is locally asymptotically stable under this condition (3.2.2.2).

A similar result to Condition (3.2.2.2) is found in [8] for the case of no immune system and a combined drug efficacy. Also, by assuming that there is no proliferation term and no antiviral therapy (i.e., $r=\varepsilon=\eta=0$), we obtain the following simplified form of Condition (3.2.2.2):

$$\frac{\beta k T_0^*}{\delta c}<1$$

which was also established in paper [36] as R_0, which is the basic reproductive number. More details about R_0 can be found in [13].

3.2.3 Successful Drug Therapy

Since it was believed that HIV may be killed by antiviral treatment, the idea of a critical drug efficacy, ε_c, was presented in [40,5]. The definition of the critical drug efficacy was observed. Thus, if the efficacy of a drug, ε, which acts to block the production of the virus from infected cells, was greater than the value of the critical drug efficacy (i.e., $\varepsilon > \varepsilon_c$), viral levels persistently decay on treatment eventually prompting eradication. If the efficacy of a drug, η, which acts to block the new infection, was less than the value of the critical drug efficacy (i.e., $\varepsilon < \varepsilon_c$), viral levels in any case would decay, but in the end, they would balance at a nonzero steady state in spite of proceeding with treatment. This discovery demonstrated that the idea of ε_c applies to HCV dynamic models in which healthy cells (target cells), *T*, levels are permitted to vary. Therefore, for the model given by (5) and its disease-free steady state condition (3.2.2.2) that described in the previous section, one can realize that the successful drug therapy, can lead to decrease in viral load and then eradicate the virus, such that:

$$\frac{1}{\delta}\left(r\left(1-\frac{T_0^*}{T_{max}}\right)+\frac{(1-\eta)(1-\varepsilon)\beta k T_0^*}{c}\right)<1$$

$$\Rightarrow \quad \frac{1}{\delta}\left(\frac{(1-\eta)(1-\varepsilon)\beta k T_0^*}{c}\right)<1-\frac{1}{\delta}\left(r\left(1-\frac{T_0^*}{T_{max}}\right)\right)$$

$$\Rightarrow \quad \left(\frac{(1-\eta)(1-\varepsilon)\beta k T_0^*}{c}\right)<\delta-r\left(1-\frac{T_0^*}{T_{max}}\right)$$

$$\Rightarrow \ \left((1-\eta)(1-\varepsilon)\beta k T_0^*\right) < c\delta - c\left(r\left(1-\frac{T_0^*}{T_{max}}\right)\right)$$

$$\Rightarrow \ (1-\eta)(1-\varepsilon) \ < \frac{c\delta - cr + \frac{crT_0^*}{T_{max}}}{\beta k T_0^*}$$

$$\Rightarrow (1-\eta)(1-\varepsilon) \ < \frac{c(\delta T_{max} - rT_{max} + rT_0^*)}{T_{max}\beta k T_0^*}$$

$$\Rightarrow \ (1-\eta)(1-\varepsilon) \ < \frac{c\delta - cr + \frac{crT_0^*}{T_{max}}}{\beta k T_0^*}$$

$$\Rightarrow (1-\eta)(1-\varepsilon) \ < \frac{c(\delta T_{max} - rT_{max} + rT_0^*)}{T_{max}\beta k T_0^*}$$

Therefore, when we fix η as a constant to be equal to η^* i.e., $\eta = \eta^*$, we obtain the value of the efficacy of a drug, ε, as follows:

$$1 - \frac{1}{1-\eta^*}\frac{c\delta T_{max} - crT_{max} + crT_0^*}{T_{max}\beta k T_0^*} \ < \ \varepsilon$$

So, the critical drug efficacy in blocking the virus production is defined as:

$$1 - \frac{1}{1-\eta^*}\frac{c\delta T_{max} - crT_{max} + crT_0^*}{T_{max}\beta k T_0^*} = \varepsilon_c \ .$$

$$\varepsilon_c < \varepsilon$$

Also, when we fix ε as a constant to be equal to ε^* i.e., $\varepsilon = \varepsilon^*$, we obtain the value of the efficacy of a drug, η, as follows:

$$1 - \frac{1}{1-\varepsilon^*}\frac{c\delta T_{max} - crT_{max} + crT_0^*}{T_{max}\beta k T_0^*} < \eta$$

So, the critical drug efficacy in reducing new infections is defined as:

$$1 - \frac{1}{1-\varepsilon^*}\frac{c\delta T_{max} - crT_{max} + crT_0^*}{T_{max}\beta k T_0^*} = \eta_c.$$

$$\eta_c < \eta$$

where T_0^* is the total number of the uninfected cells. We found that the values of the efficacy of a drug ε and η are required to be greater than the values of the critical drug efficacy ε_c (i.e., $\varepsilon_c < \varepsilon$ and $\eta_c < \eta$) for successful antiviral therapy tends to decrease in viral load and then eradicate the virus.

CHAPTER 4

NUMERICAL SIMULATIONS

In this chapter, we use numerical solutions to illustrate the theoretical results that were defined in Chapter 3 for model (5), to show the drug effectiveness, and to compare our model (5) with other models. Parameter values have been chosen from [36, 8] to give an illustration of the behavior of the model (5). The numerical values depend on the particular units that are chosen, which have been discussed in Chapter 3. We use the same values of the parameters, as shown in Table 2, in all numerical simulations.

Table 2: The values of parameters.

Parameters	Values
T_{max}	1.0*10^(7)
s	1.0*10^(5)
r	0.1
d	1.0*10^(-2)
β	2.0*10^(-7)
δ	1.0*10^(-1)
p	6.4*10^(-4)
k	4.0*10^(0)
c	5.0*10^(0)
q	2.0*10^(0)

μ	4.4*10^(-7)
b	1.0*10^(-2)
g	1.0*10^(-5)
h	1*10^(-2)
ε	0.7-0.9
η	0.7-0.9

4.1 Disease-Free Equilibrium Simulations

For numerical solutions of the model (5), we run simulations using the parameter values listed in Table 2 that guarantee condition (3.2.2.2) is satisfied, and the initial conditions: T= 1.0*10^(4), I=2.0*10^(0), V= 3.0*10^(0), Z=1.0*10^(0), and W=1.5*10^(0). The numerical simulation results are presented in Figure 8(a, b, c, d) and show that the uninfected cells $T(t)$ converge to $T_0^* = \frac{T_{max}}{2r}\left[r - d + \sqrt{(r-d)^2 + \frac{4rs}{T_{max}}}\right] = 10^6$ while the other four populations converge to zero. Therefore, the disease-free equilibrium is locally asymptotically stable under condition (3.2.2.2).

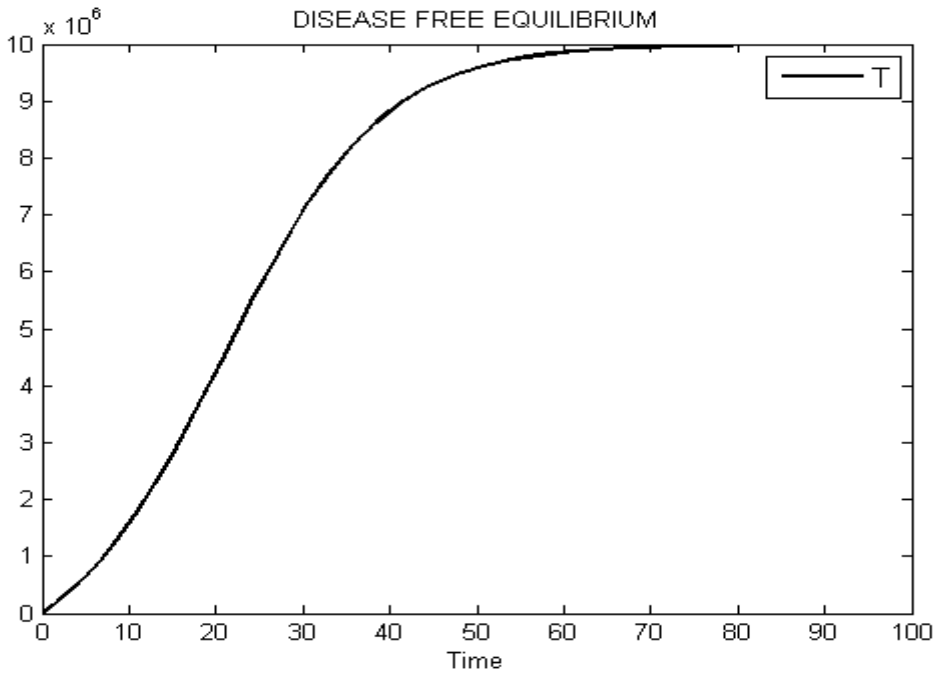

Figure 8a: Numerical solution curve for the uninfected cells in 100 days.

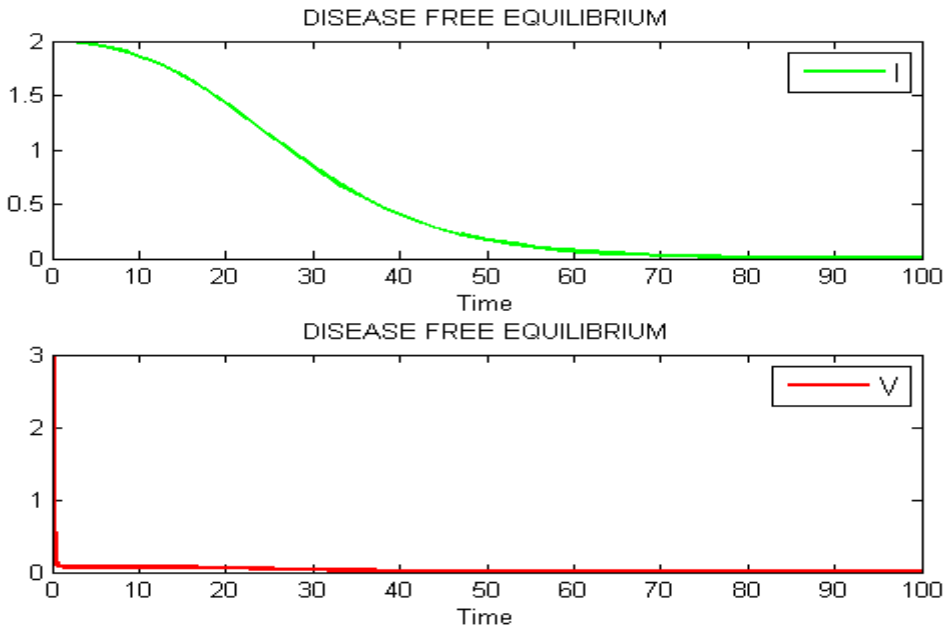

Figure 8b: Numerical solution curve for the infected cells and virus particles in 100 days.

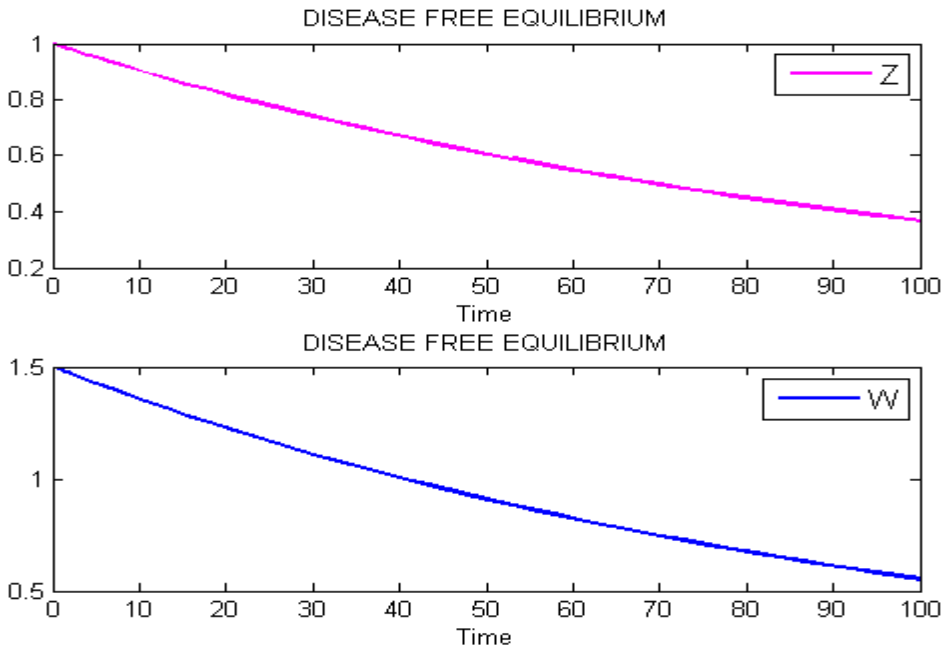

Figure 8c: Numerical solution curve for the CTLs and the antibody responses in 100 days.

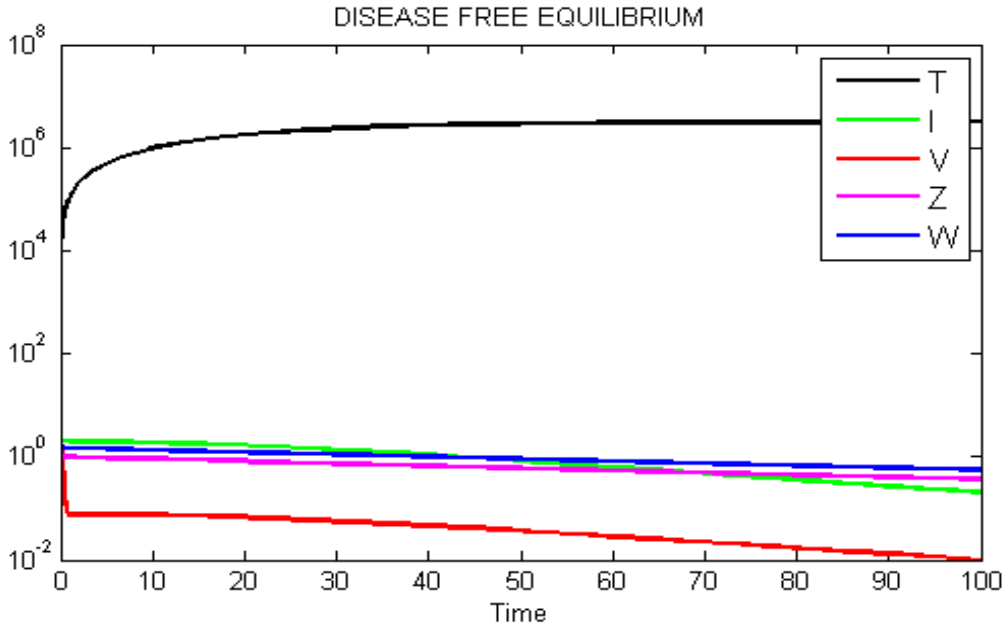

Figure 8d: Numerical simulation of the HCV model in 100 days.

4.2 System Behavior with no Immune Responses and no Drug (i.e., q=p=η=ε=0).

We run simulations using again the parameter values listed in Table 2 but in the absence of immune responses and drug i.e., q=p=η=ε=0. Therefore, condition (3.2.2.2) is not satisfied. We use the initial conditions: T= 1.0*10^(4), I=2.0*10^(0), V= 3.0*10^(0), Z=1.0*10^(0), and W=1.5*10^(0). The numerical simulation results are presented in Figure 9(a, b, c, d) and show that the uninfected cells $T(t)$ do not converge to $T_0^* = \frac{T_{max}}{2r}\left[r - d + \sqrt{(r-d)^2 + \frac{4rs}{T_{max}}}\right] = 10^6$ and the other four populations do not converge to zero. Therefore, the disease-free equilibrium is unstable.

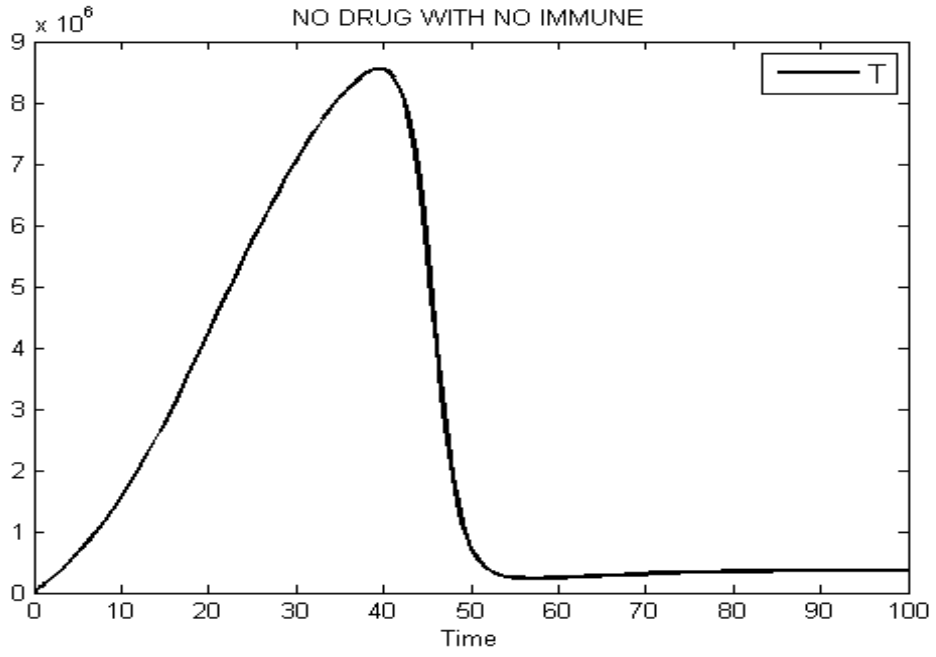

Figure 9a: Numerical solution curve for the uninfected cells in 100 days.

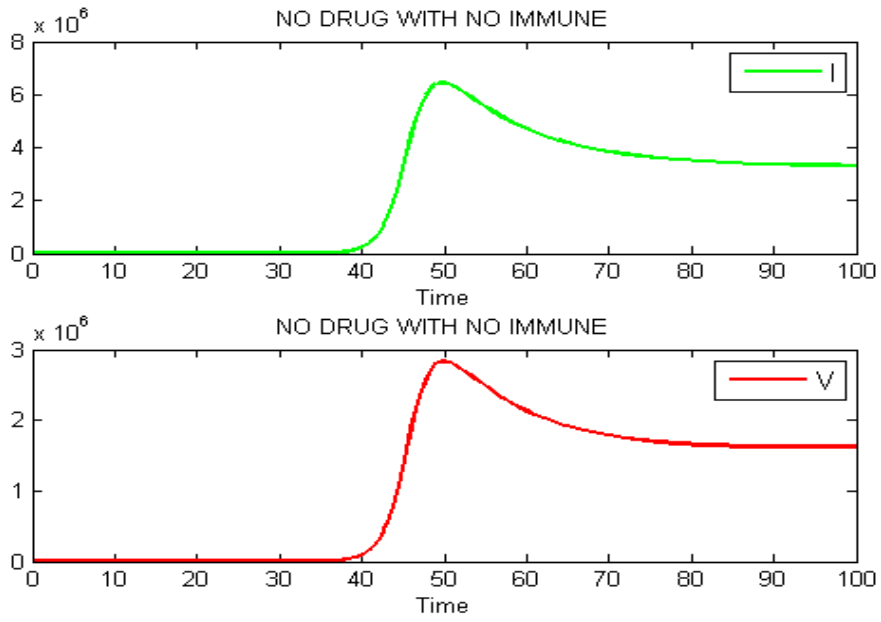

Figure 9b: Numerical solution curve for the infected cells and free virus in 100 days.

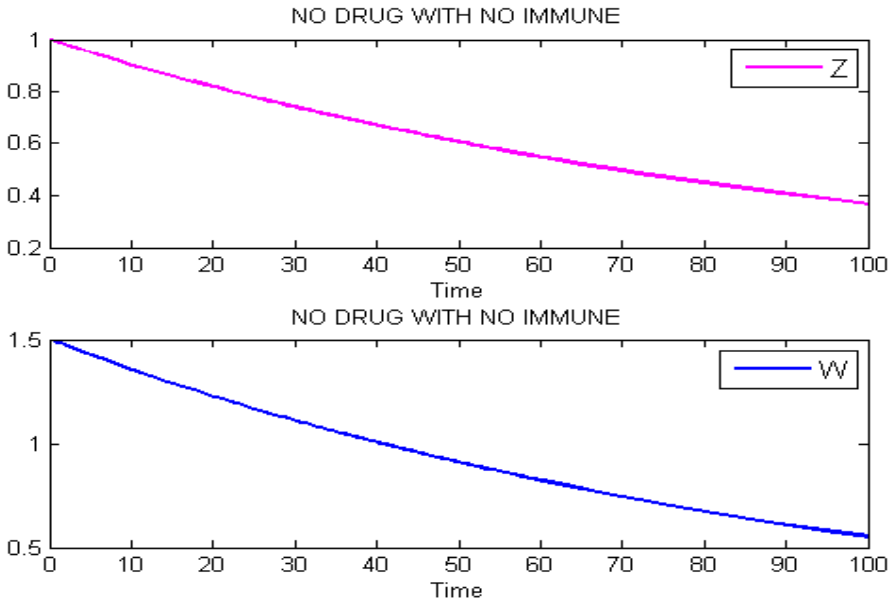

Figure 9c: Numerical solution curve for the CTLs and the antibody responses in 100 days.

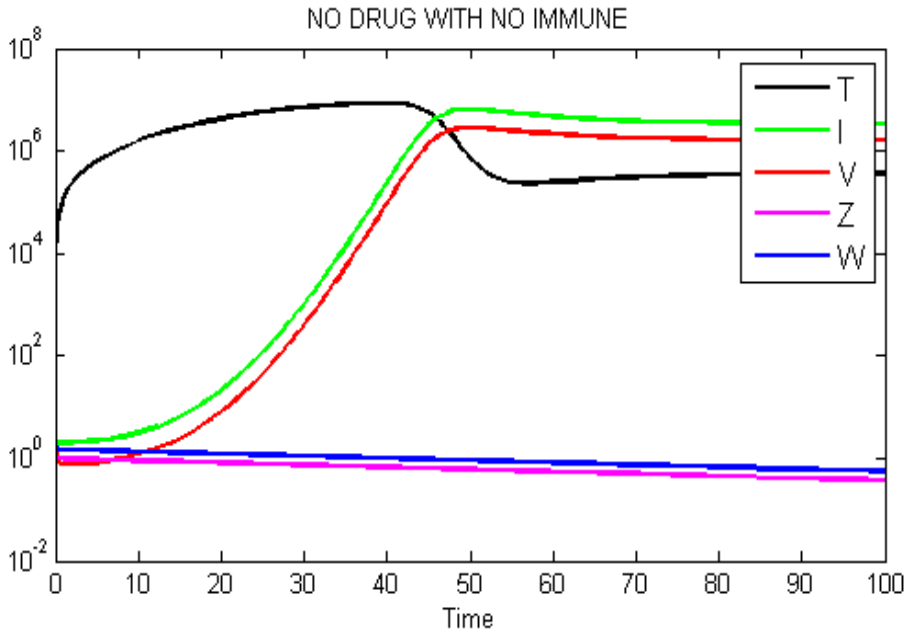

Figure 9d: Numerical simulation of the HCV model in 100 days.

4.3 System Behavior with Drug but no Immune Responses (i.e., q=p=0; η=ε=0.9).

We run simulations using the initial conditions: T= 1.0*10^(4), I=2.0*10^(0), V= 3.0*10^(0), Z=1.0*10^(0), and W=1.5*10^(0) and the parameter values listed in Table 2, but in the absence of immune responses i.e., q=p=0. When drug acts to block both the new HCV infections and the production or release of viruses by infected cells, I, i.e., η=ε=0.9, then condition (3.2.2.2) is satisfied. The numerical simulation results are presented in Figure 10(a, b, c, d) and show that the uninfected cells $T(t)$ converge to $T_0^* = \frac{T_{max}}{2r}\left[r - d + \sqrt{(r-d)^2 + \frac{4rs}{T_{max}}}\right] = 10^6$ while the other four populations converge to zero. Therefore, the disease-free equilibrium is locally asymptotically stable.

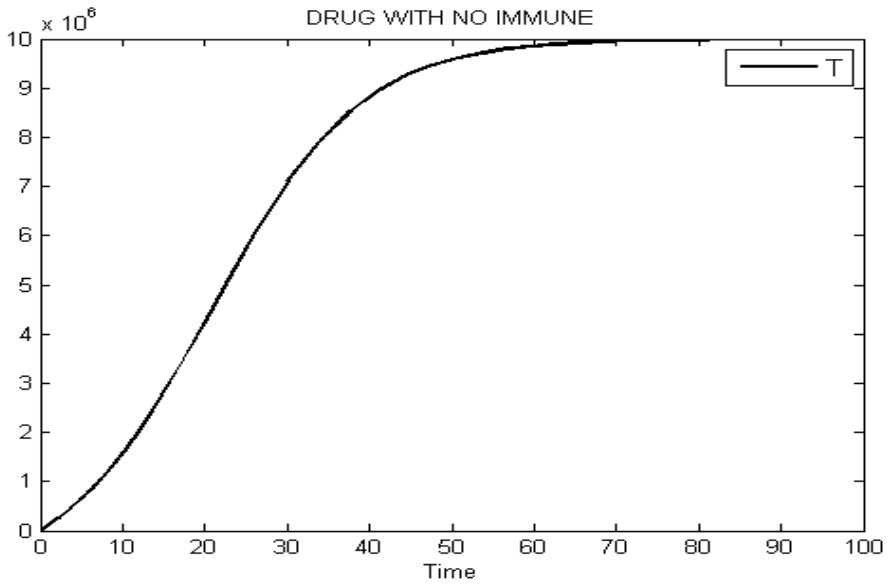

Figure 10a: Numerical solution curve for the uninfected cells in 100 days.

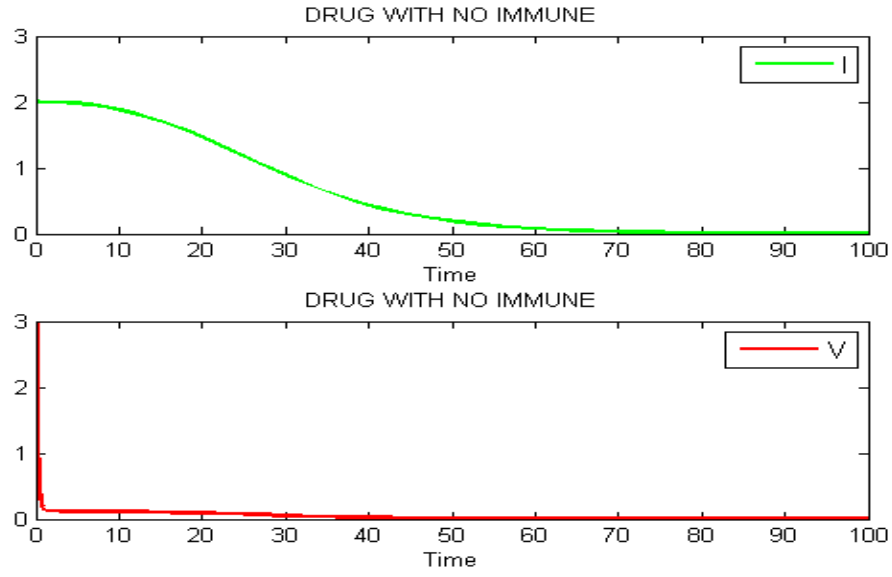

Figure 10b: Numerical solution curve for the infected cells and the free virus in 100 days.

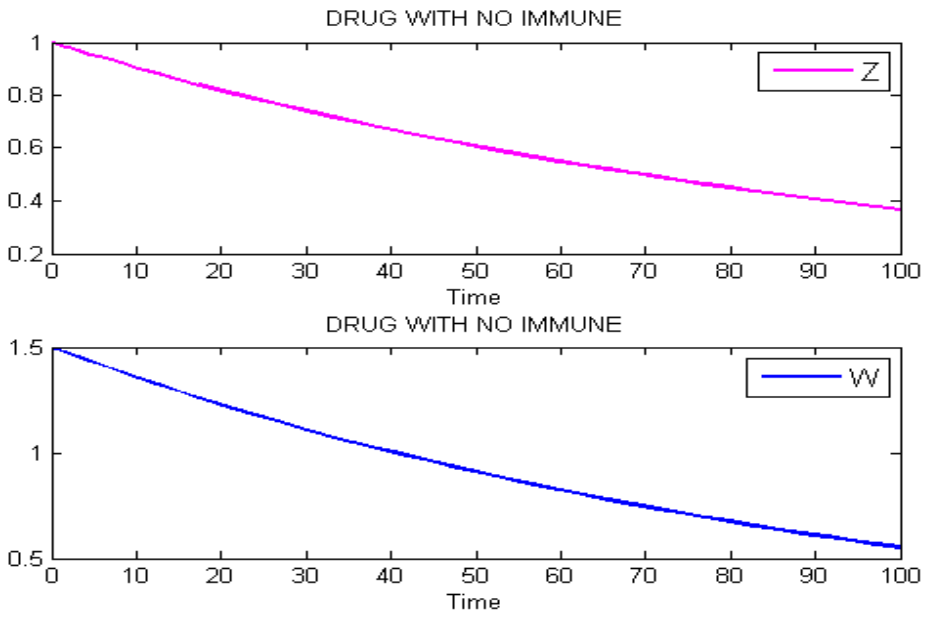

Figure 10c: Numerical solution curve for the CTLs and the antibody responses in 100 days.

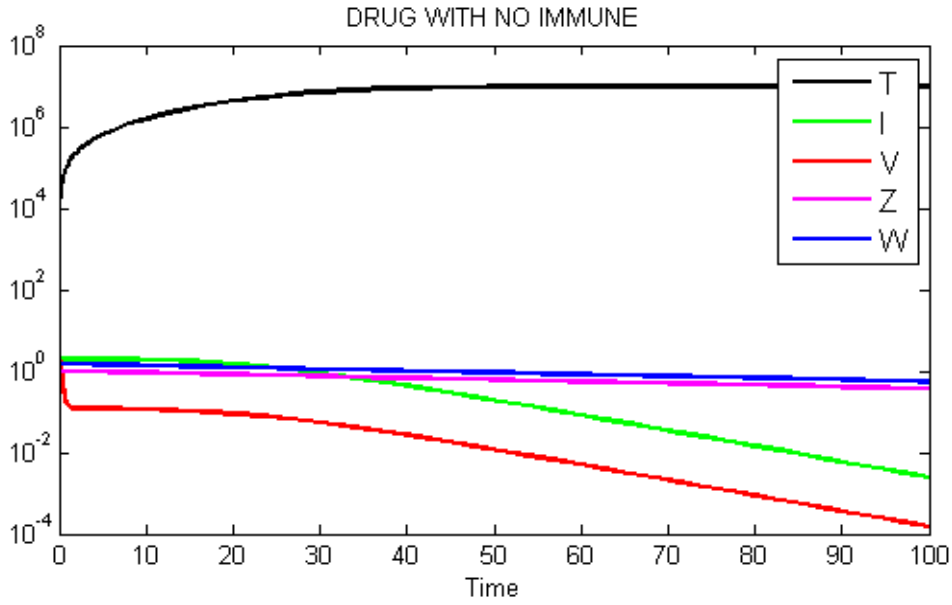

Figure 10d: Numerical simulation of the HCV model in 100 days.

4.4 System Behavior with Drug and no Immune Responses (i.e., $q=p=0$; $\eta=0.9, \varepsilon=0$).

We run simulations using the initial conditions: T= 1.0*10^(4), I=2.0*10^(0), V= 3.0*10^(0), Z=1.0*10^(0), and W=1.5*10^(0) and the parameter values listed in Table 2, but in the absence of immune responses i.e., $q=p=0$. When drug acts to block new HCV infections ($\eta=0.9$, $\varepsilon=0$), then condition (3.2.2.2) is not satisfied. The numerical simulation results are presented in Figure 11(a, b, c, d) and show that the uninfected cells $T(t)$ do not converge to $T_0^* = \frac{T_{max}}{2r}\left[r - d + \sqrt{(r-d)^2 + \frac{4rs}{T_{max}}}\right] = 10^6$ and the other four populations do not converge to zero. Therefore, the disease-free equilibrium is unstable.

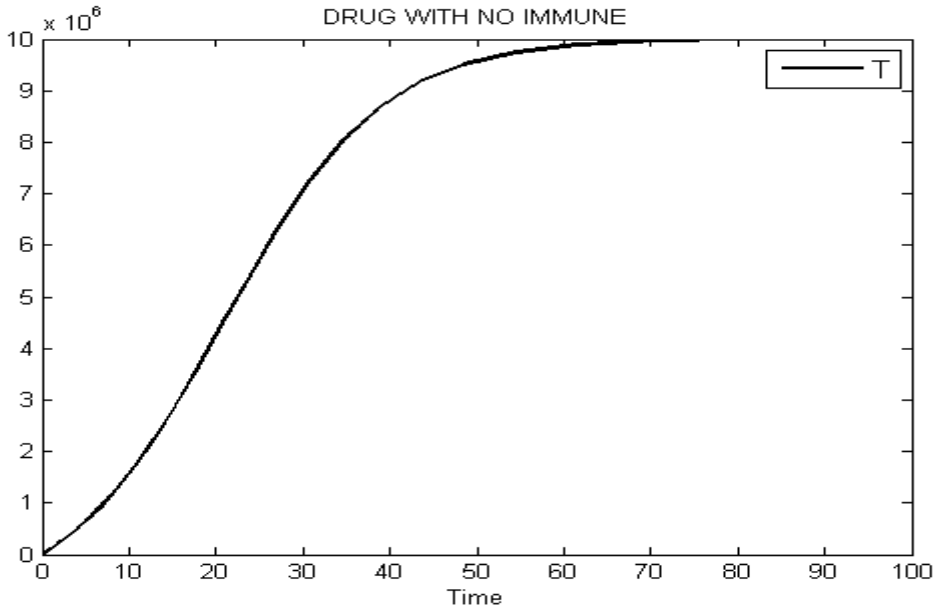

Figure 11a: Numerical solution curve for the uninfected cells in 100 days.

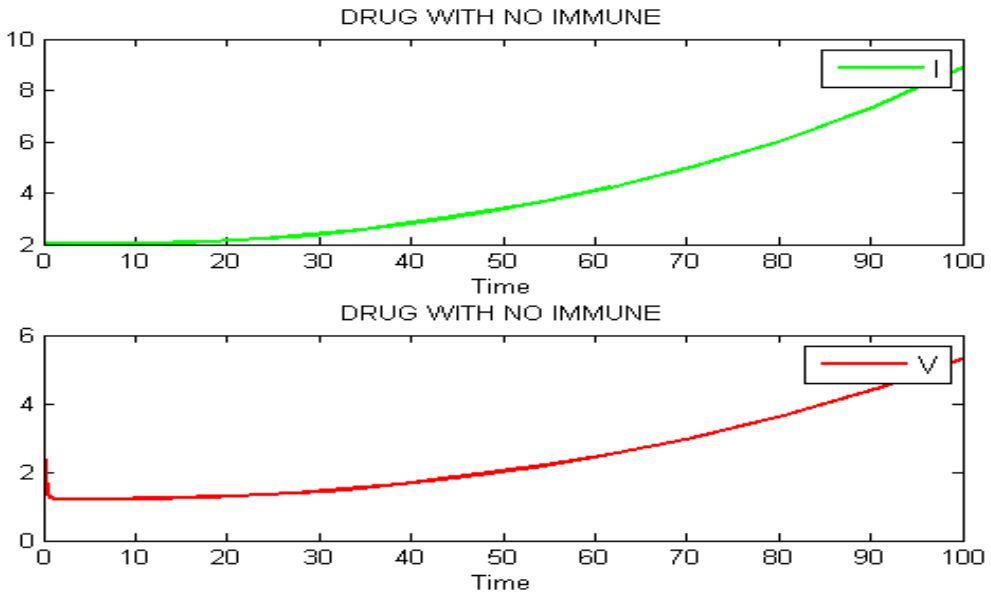

Figure 11b: Numerical solution curve for the infected cells and the free virus in 100 days.

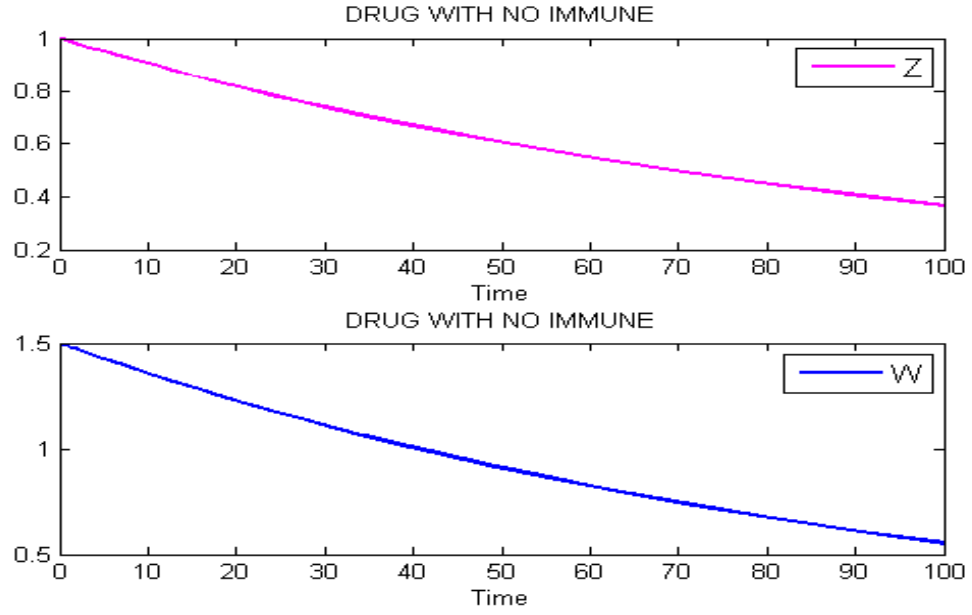

Figure 11c: Numerical solution curve for the CTLs and the antibody responses in 100 days.

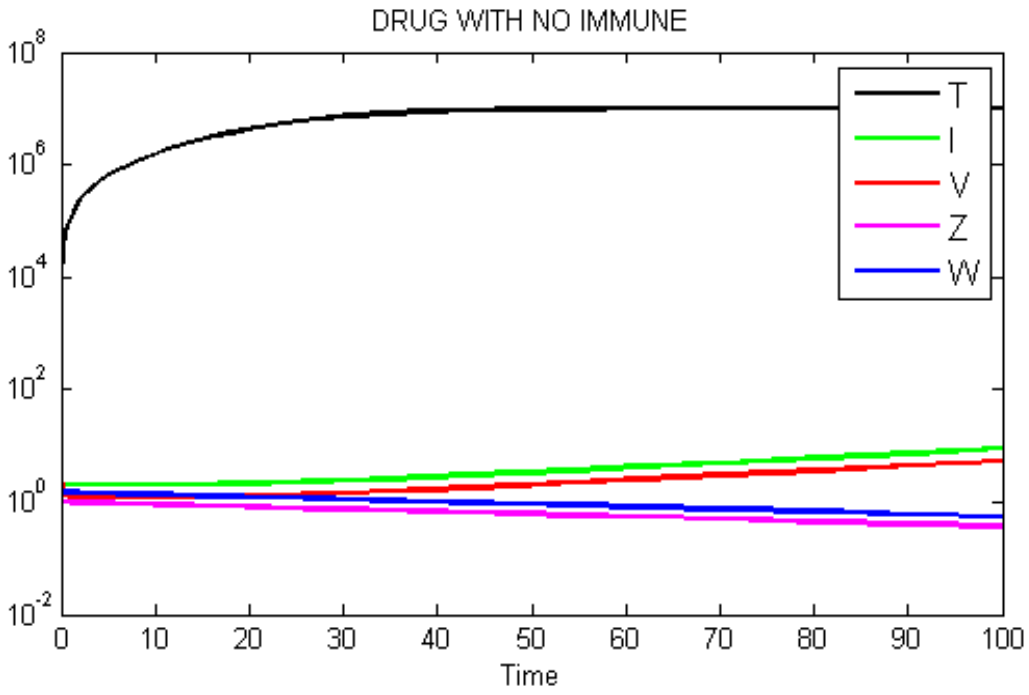

Figure 11d: Numerical simulation of the HCV model in 100 days.

4.5 System Behavior with Drug but no Immune Responses (i.e., q=p=0; η=0, ε=0.9).

We run simulations using the initial conditions: T= 1.0*10^(4), I=2.0*10^(0), V= 3.0*10^(0), Z=1.0*10^(0), and W=1.5*10^(0) and the parameter values listed in Table 2, but in the absence of immune responses i.e., q=p=0. When drug acts to block the production or release of viruses by infected cells, I, i.e., η=0, ε=0.9, then condition (3.2.2.2) is not satisfied. The numerical simulation results are presented in Figure 12(a, b, c, d) and show that the uninfected cells $T(t)$ do not converge to $T_0^* = \frac{T_{max}}{2r}\left[r - d + \sqrt{(r-d)^2 + \frac{4rs}{T_{max}}}\right] = 10^6$ and the other four populations do not converge to zero. Therefore, the disease-free equilibrium is unstable.

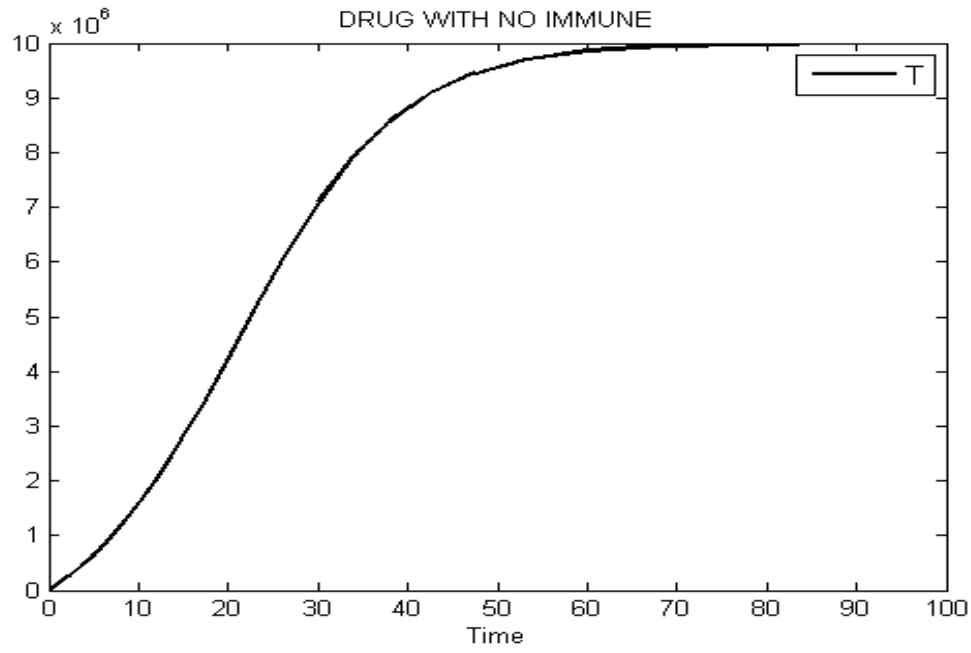

Figure 12a: Numerical solution curve for the uninfected cells in 100 days.

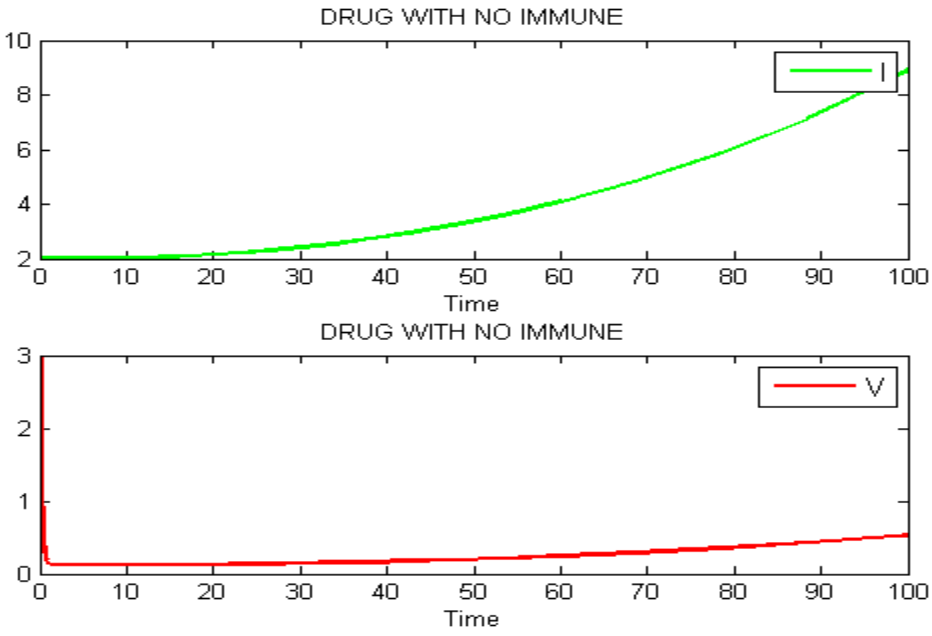

Figure 12b: Numerical solution curve for the infected cells and the free virus in 100 days.

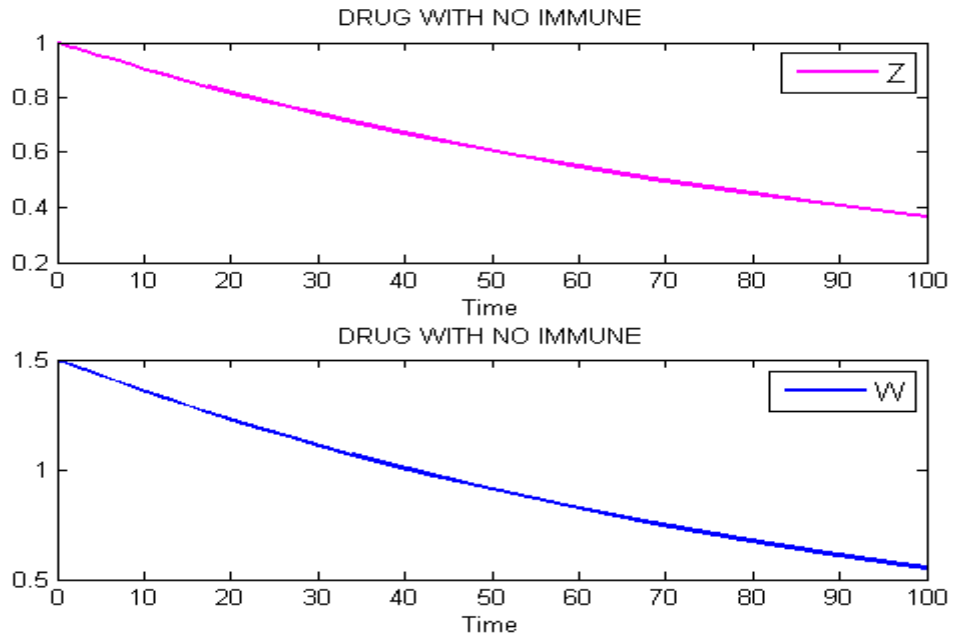

Figure 12c: Numerical solution curve for the CTLs and the antibody responses in 100 days.

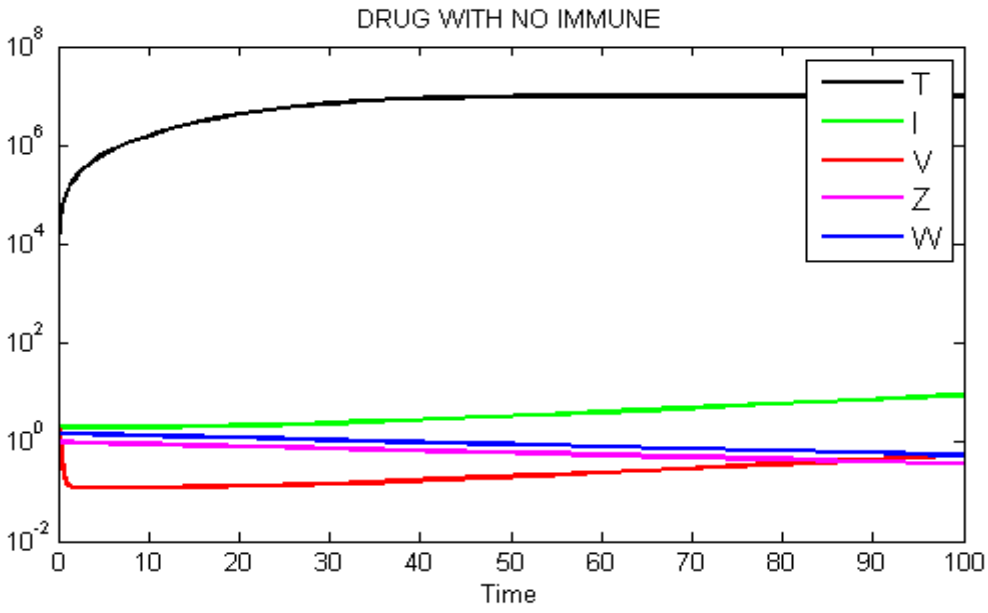

Figure 12d: Numerical simulation of the HCV model in 100 days.

4.6 System Behavior with Drug and no Immune Responses (i.e., $q=p=0$; η=0.7, ε=0.8).

We run simulations using the initial conditions: T= 1.0*10^(4), I=2.0*10^(0), V= 3.0*10^(0), Z=1.0*10^(0), and W=1.5*10^(0) and the parameter values listed in Table 2, but in the absence of immune responses i.e., $q=p=0$. When drug acts to block both the new HCV infections and the production or release of viruses by infected cells, I, i.e., η=0.7, ε=0.8, then condition (3.2.2.2) is satisfied. The numerical simulation results are presented in Figure 13(a, b, c, d) and show that the uninfected cells $T(t)$ converge to $T_0^* = \frac{T_{max}}{2r}\left[r - d + \sqrt{(r-d)^2 + \frac{4rs}{T_{max}}}\right] = 10^6$ while the other four populations converge to zero. Therefore, the disease-free equilibrium is stable.

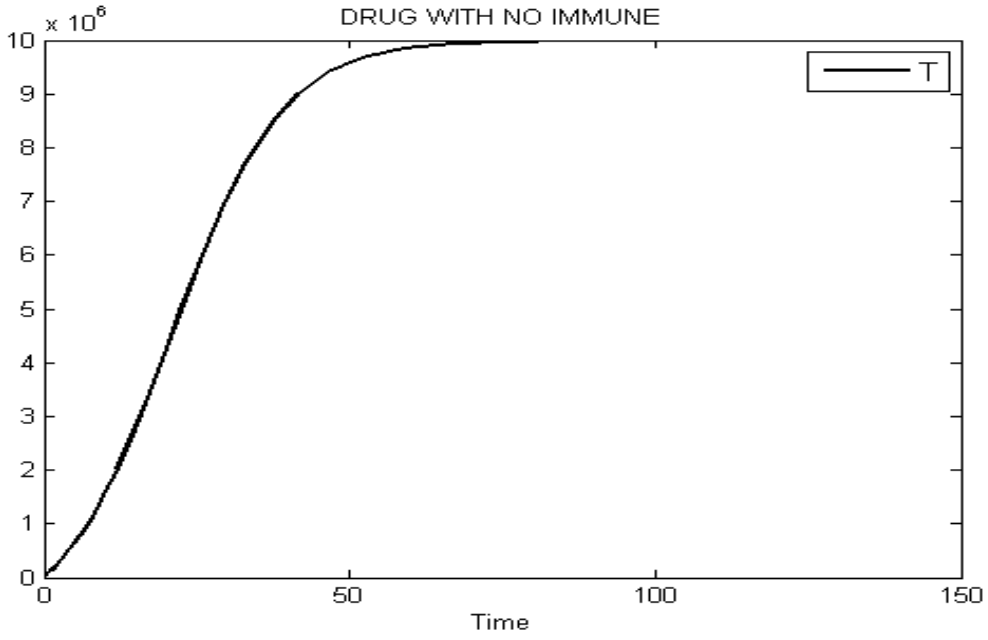

Figure 13a: Numerical solution curve for the uninfected cells in 150 days.

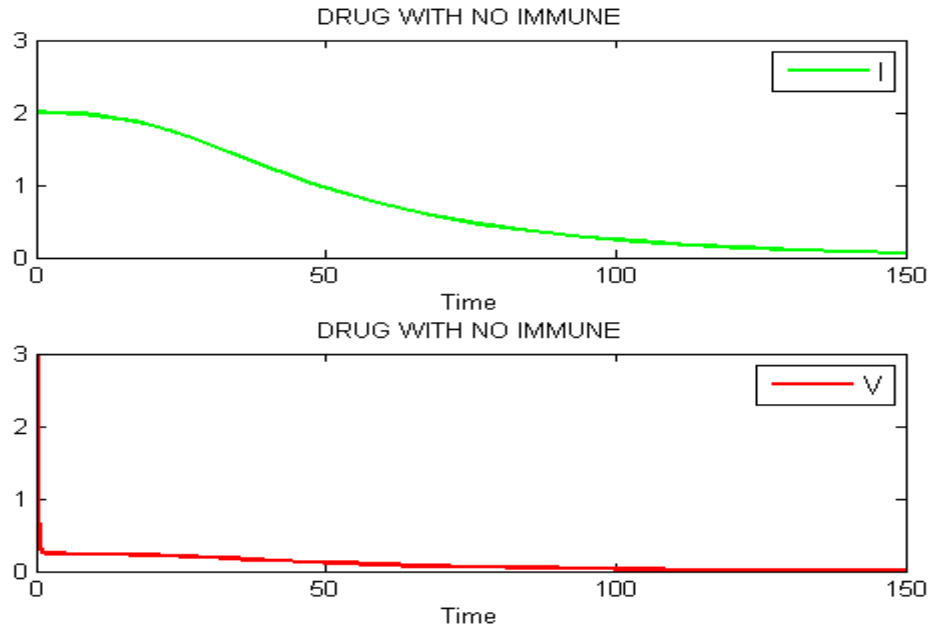

Figure 13b: Numerical solution curve for the infected cells and free virus in 150 days.

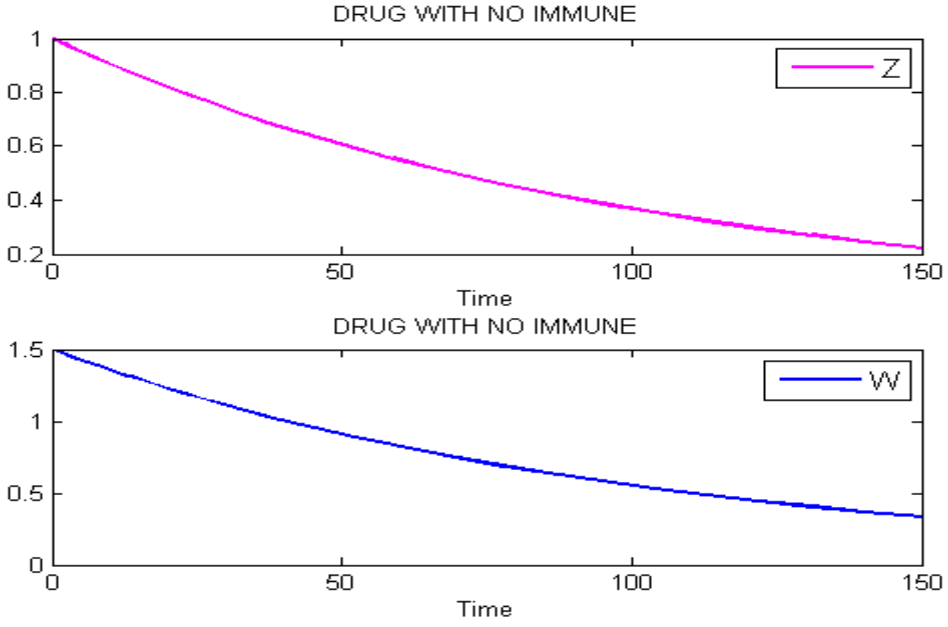

Figure 13c: Numerical solution curve for the CTLs and the antibody responses in 150 days.

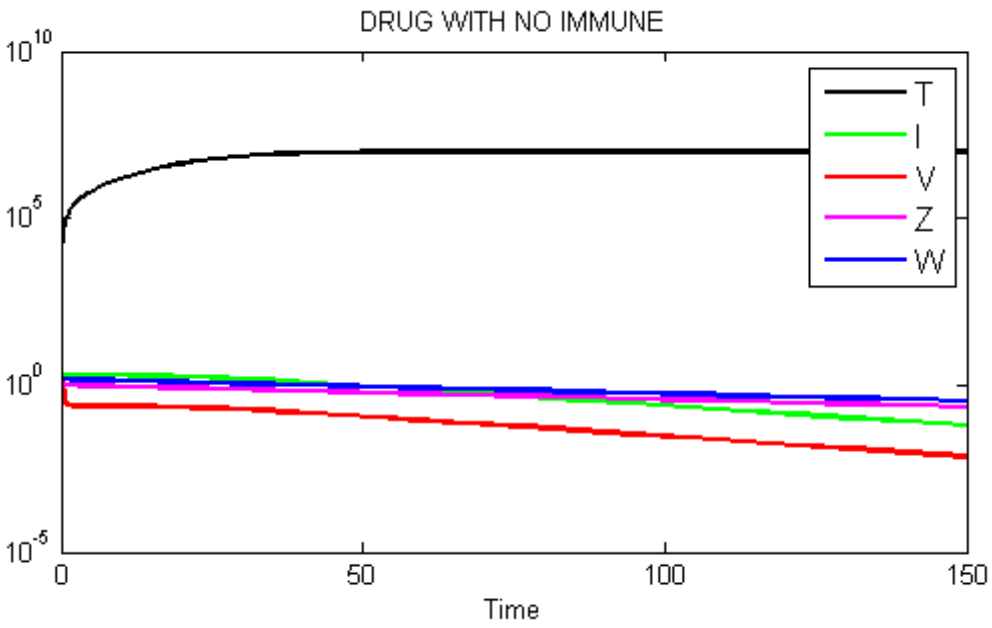

Figure 13d: Numerical simulation of the HCV model in 150 days.

4.7 System Behavior with Drug and no Immune Responses (i.e., q=p=0; η=0.8, ε=0.6).

We run simulations using the initial conditions: T= 1.0*10^(4), I=2.0*10^(0), V= 3.0*10^(0), Z=1.0*10^(0), and W=1.5*10^(0) and the parameter values listed in Table 2, but in the absence of immune responses i.e., q=p=0. When drug acts to block both the new HCV infections and the production or release of viruses by infected cells, I, i.e., η=0.8, ε=0.6), then condition (3.2.2.2) is satisfied. The numerical simulation results are presented in Figure 14(a, b, c, d) and show that the uninfected cells $T(t)$ converge to $T_0^* = \frac{T_{max}}{2r}\left[r - d + \sqrt{(r-d)^2 + \frac{4rs}{T_{max}}}\right] = 10^6$ while the other four populations converge to zero. Therefore, the disease-free equilibrium is stable.

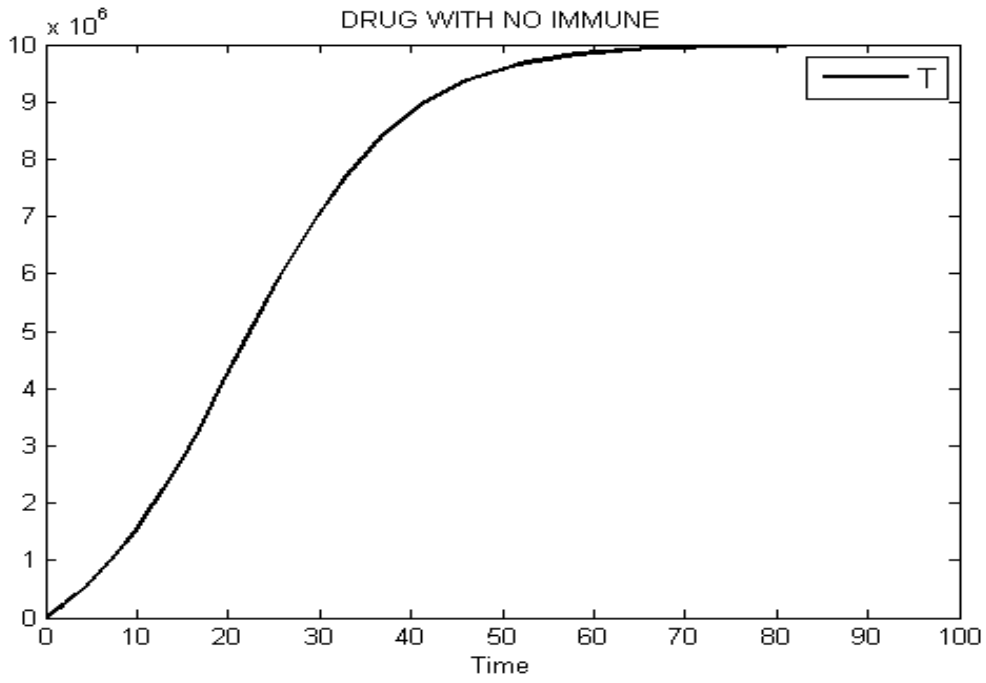

Figure 14a: Numerical solution curve for the uninfected cells in 100 days.

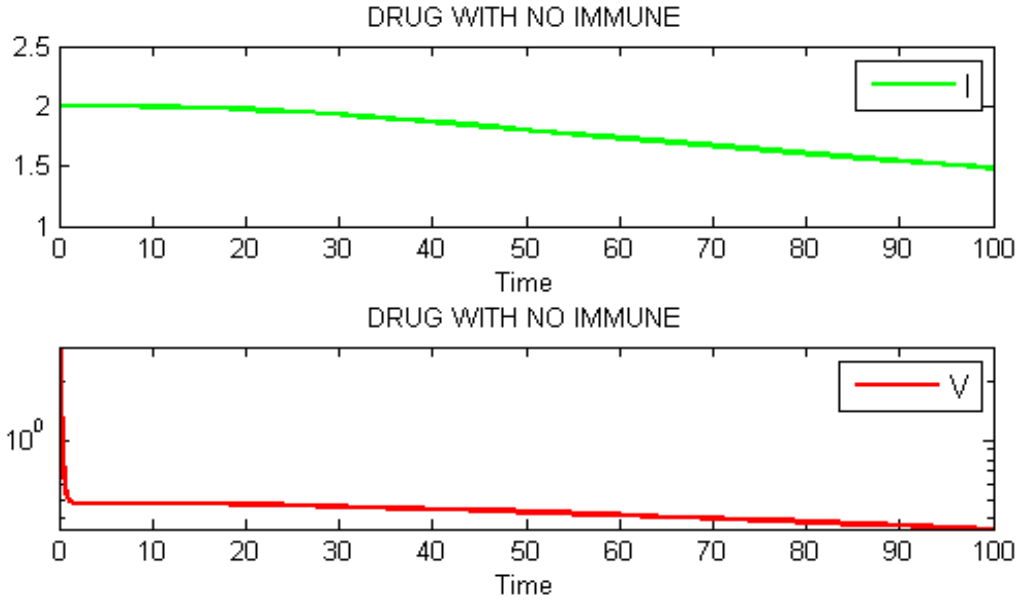

Figure 14b: Numerical solution curve for the infected cells and free virus in 100 days.

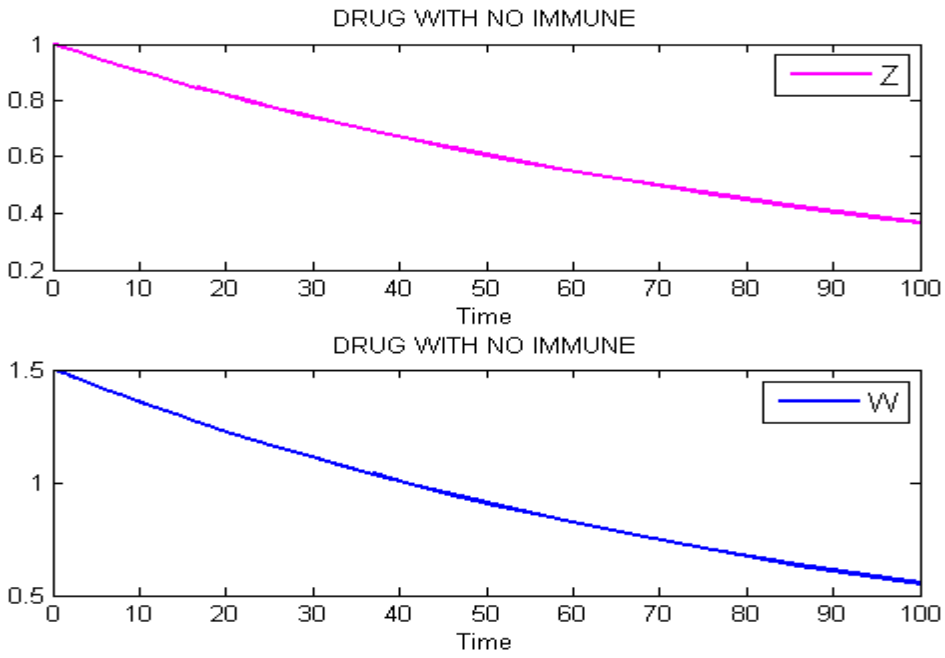

Figure 14c: Numerical solution curve for the CTLs and the antibody responses in 100 days.

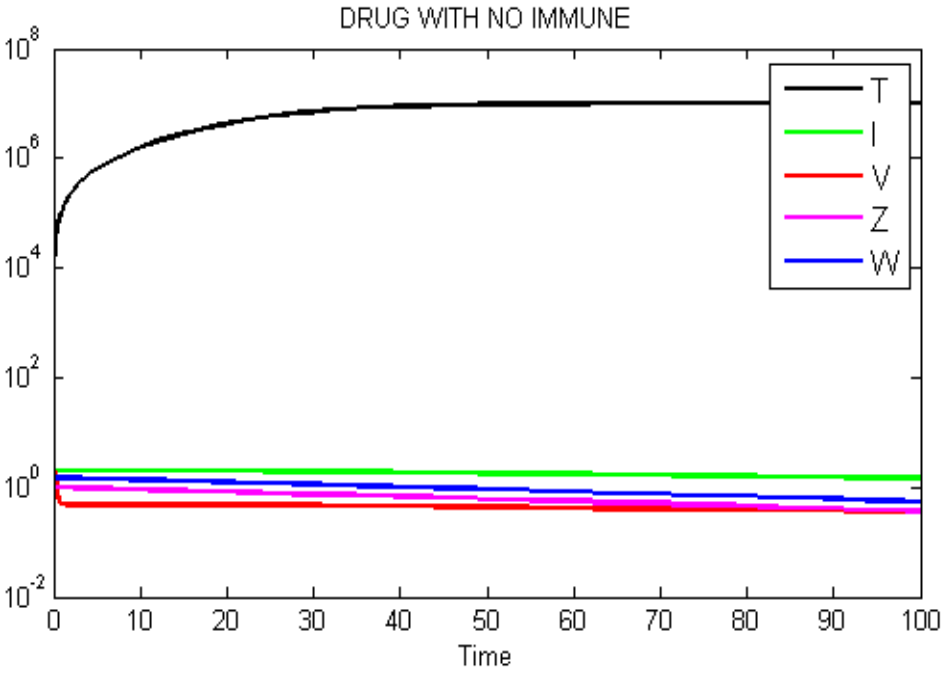

Figure 14d: Numerical simulation of the HCV model in 100 days.

4.8 System Behavior with Drug and no Immune Responses (i.e., $q=p=0$; η=0.7, ε=0.6).

We run simulations using the initial conditions: T= 1.0*10^(4), I=2.0*10^(0), V= 3.0*10^(0), Z=1.0*10^(0), and W=1.5*10^(0) and the parameter values listed in Table 2, but in the absence of immune responses i.e., $q=p=0$. When drug acts to block both the new HCV infections and the production or release of viruses by infected cells, I, i.e., η=0.7, ε=0.6, then condition (3.2.2.2) is not satisfied. The numerical simulation results are presented in Figure 15(a, b, c, d) and show that the uninfected cells $T(t)$ do not converge to $T_0^* = \frac{T_{max}}{2r}\left[r - d + \sqrt{(r-d)^2 + \frac{4rs}{T_{max}}}\right] = 10^6$ and the other four populations do not converge to zero. Therefore, the disease-free equilibrium is unstable.

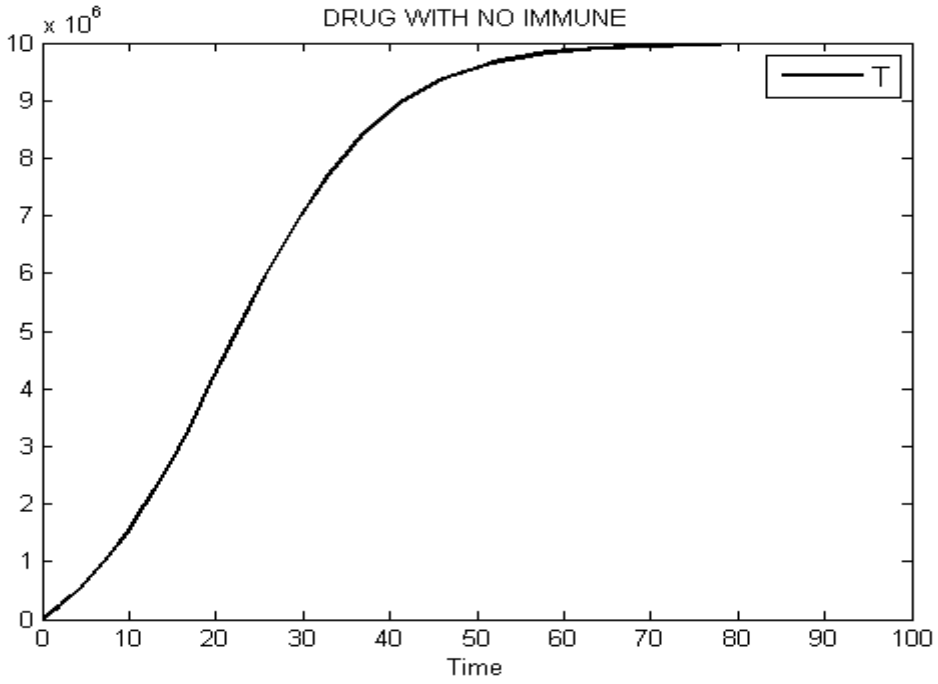

Figure 15a: Numerical solution curve for the uninfected cells in 100 days.

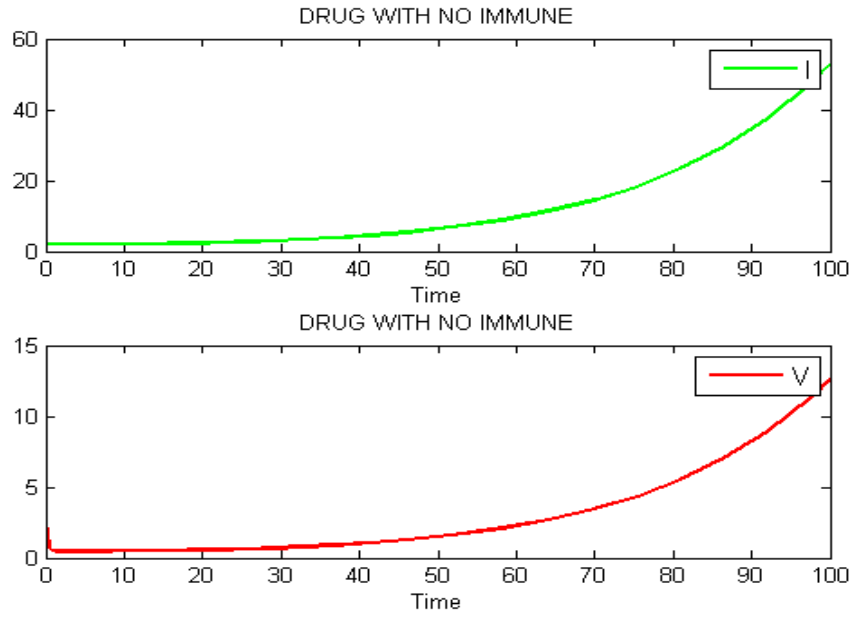

Figure 15b: Numerical solution curve for the infected cells and free virus in 100 days.

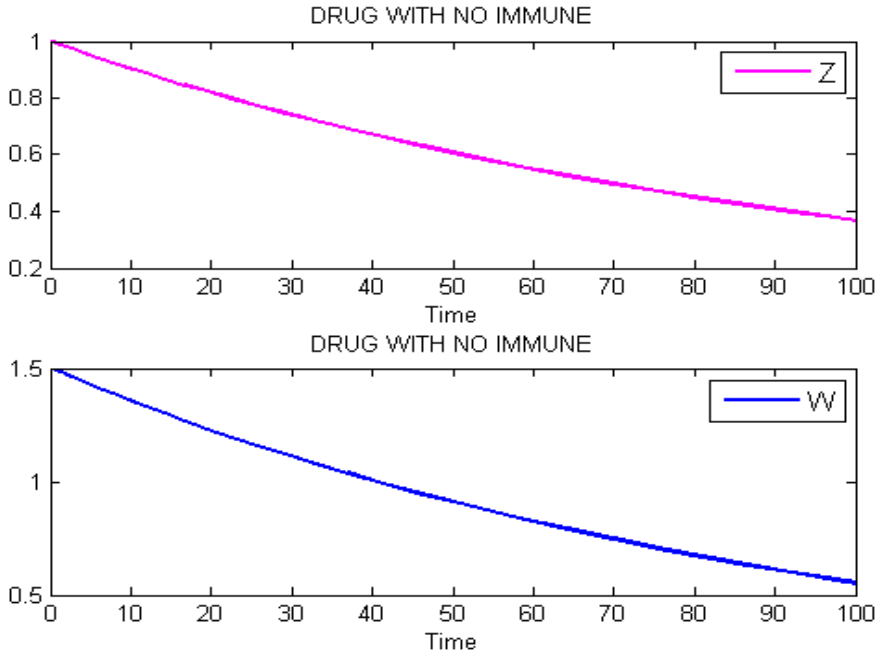

Figure 15c: Numerical solution curve for the CTLs and the antibody responses in 100 days.

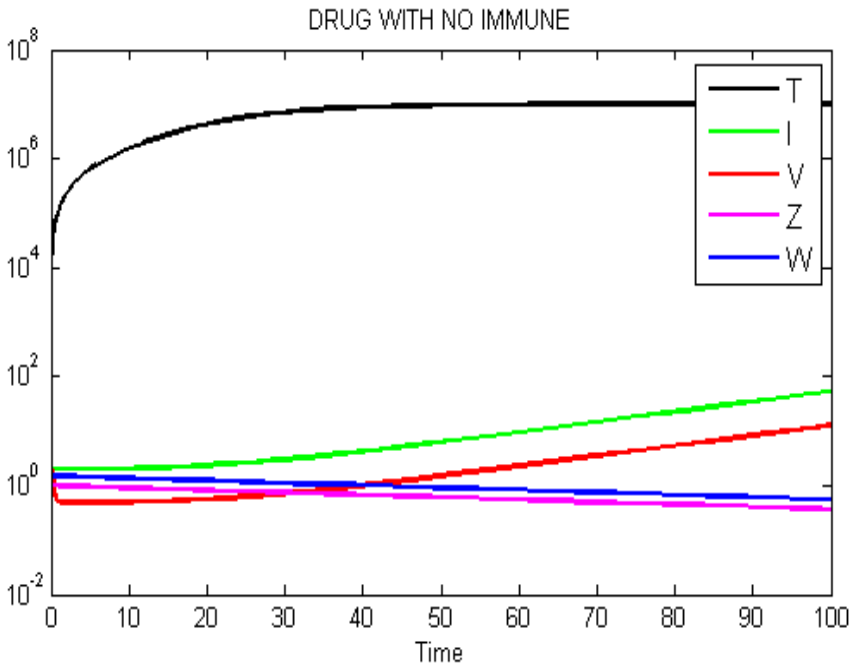

Figure 15d: Numerical simulation of the HCV model in 100 days.

4.9 Increase the Cell Proliferation Rate (i.e., r=0.5) with Immune Responses and Drug.

We run simulations using the initial conditions: T= 1.0*10^(4), I=2.0*10^(0), V= 3.0*10^(0), Z=1.0*10^(0), and W=1.5*10^(0) and the parameter values listed in Table 2. By increasing the cell proliferation rate i.e., r=0.5, then condition (3.2.2.2) is not satisfied. The numerical simulation results with drug i.e., η=0.8, ε=0.7 are presented in Figure 16(a, b, c, d) and show that the uninfected cells $T(t)$ do not converge to $T_0^* = \frac{T_{max}}{2r}\left[r - d + \sqrt{(r-d)^2 + \frac{4rs}{T_{max}}}\right] = 10^6$ and the other four populations do not converge to zero. Therefore, the disease-free equilibrium is unstable.

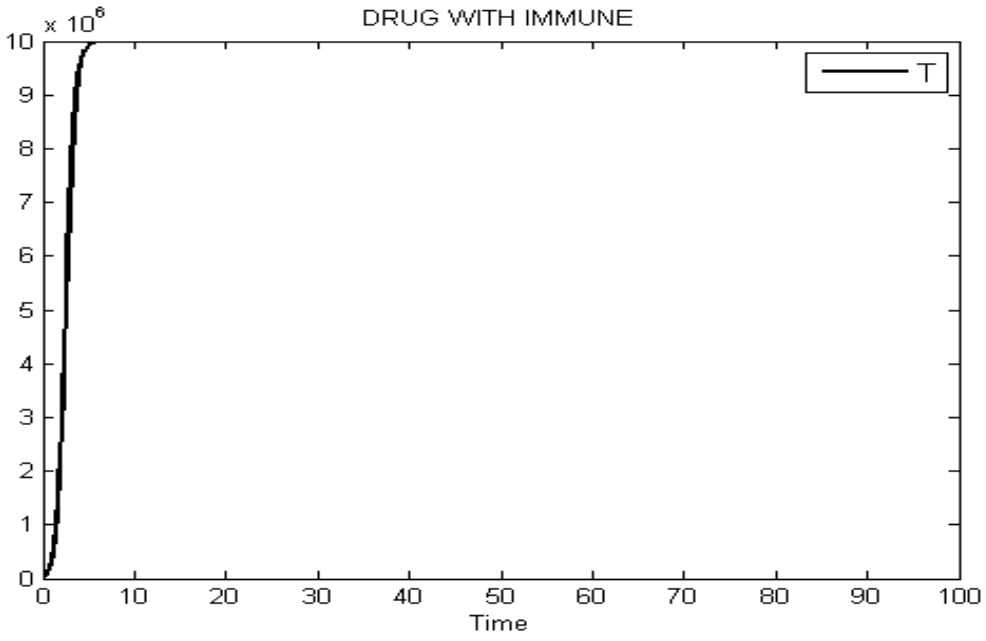

Figure 16a: Numerical solution curve for the uninfected cells in 150 days.

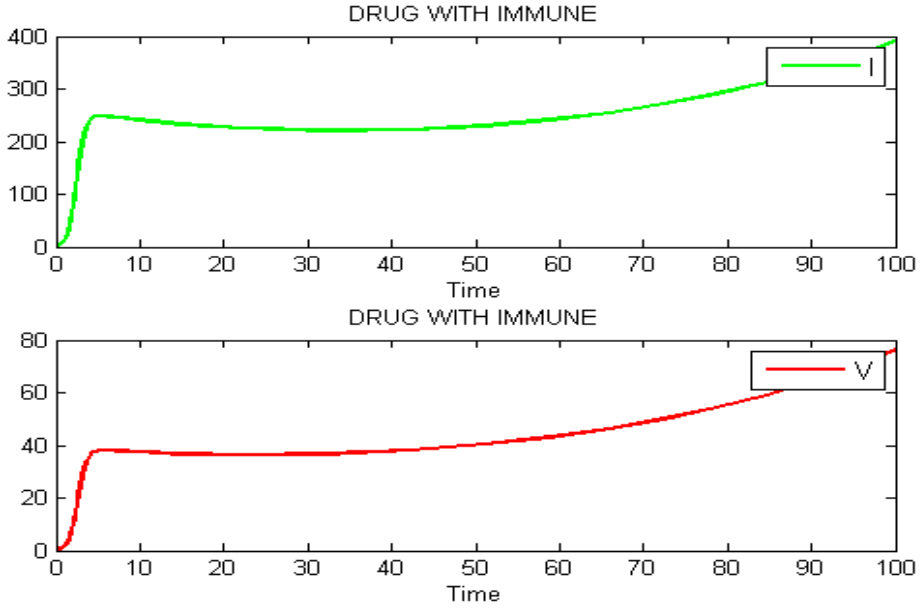

Figure 16b: Numerical solution curve for the infected cells and free virus in 150 days.

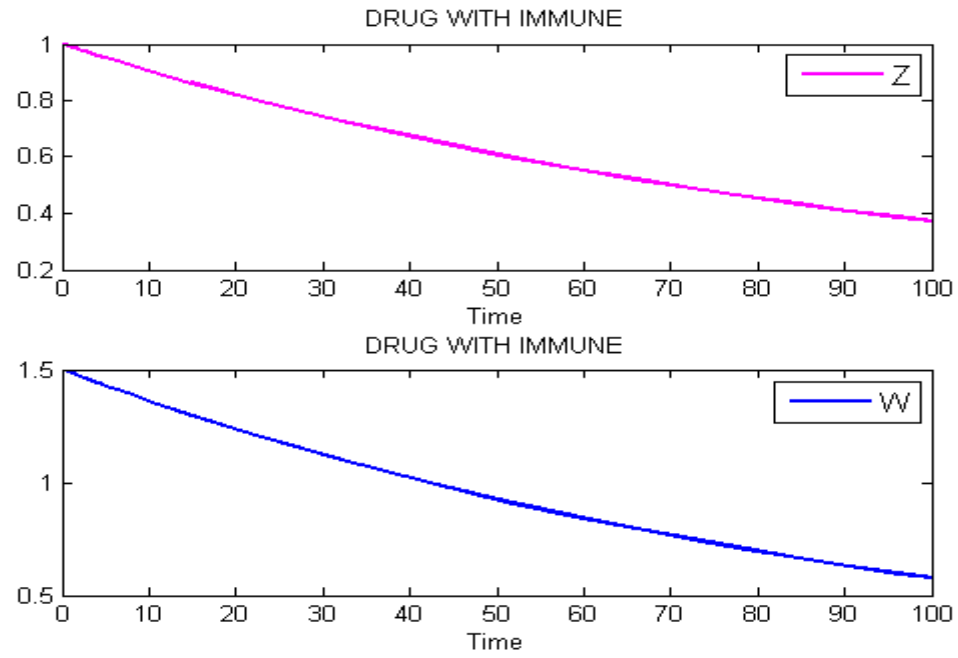

Figure 16c: Numerical solution curve for the CTLs and the antibody responses in 150 days.

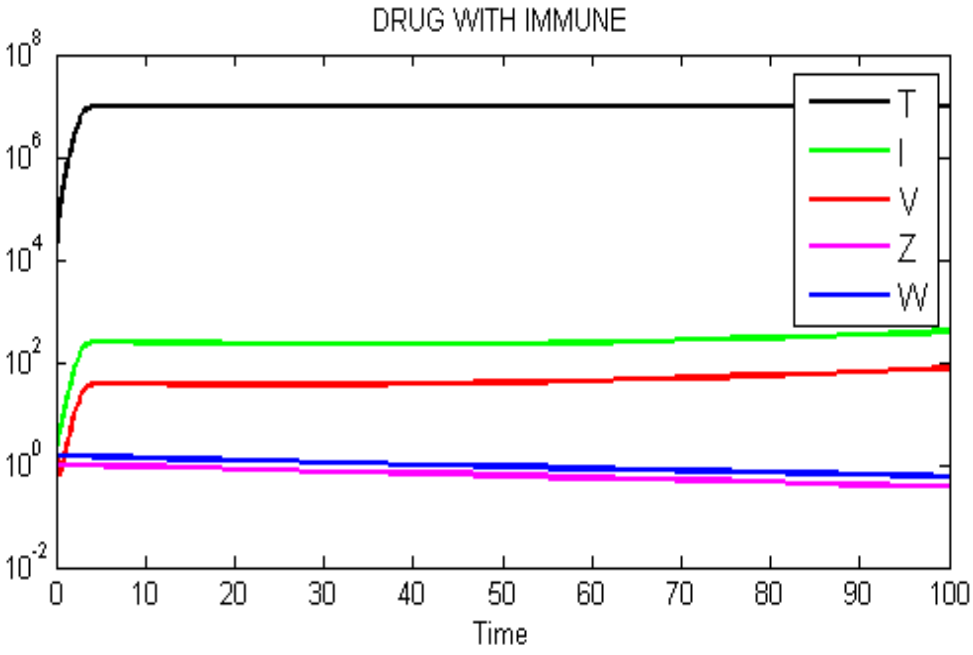

Figure 16d: Numerical simulation of the HCV model in 150 days.

4.10 Increase the Cell Proliferation Rate (i.e., r=2) with Immune Responses and Drug.

We run simulations using the initial conditions: T= 1.0*10^(4), I=2.0*10^(0), V= 3.0*10^(0), Z=1.0*10^(0), and W=1.5*10^(0) and the parameter values listed in Table 2. By increasing the cell proliferation rate i.e., r=0.2, then condition (3.2.2.2) is not satisfied. The numerical simulation results with drug i.e., η=0.7, ε=0.7 are presented in Figure 17(a, b, c, d) and show that the uninfected cells $T(t)$ does not converge to $T_0^* = \frac{T_{max}}{2r}\left[r - d + \sqrt{(r-d)^2 + \frac{4rs}{T_{max}}}\right] = 10^6$ and the other four populations do not converge to zero. Therefore, the disease-free equilibrium is unstable.

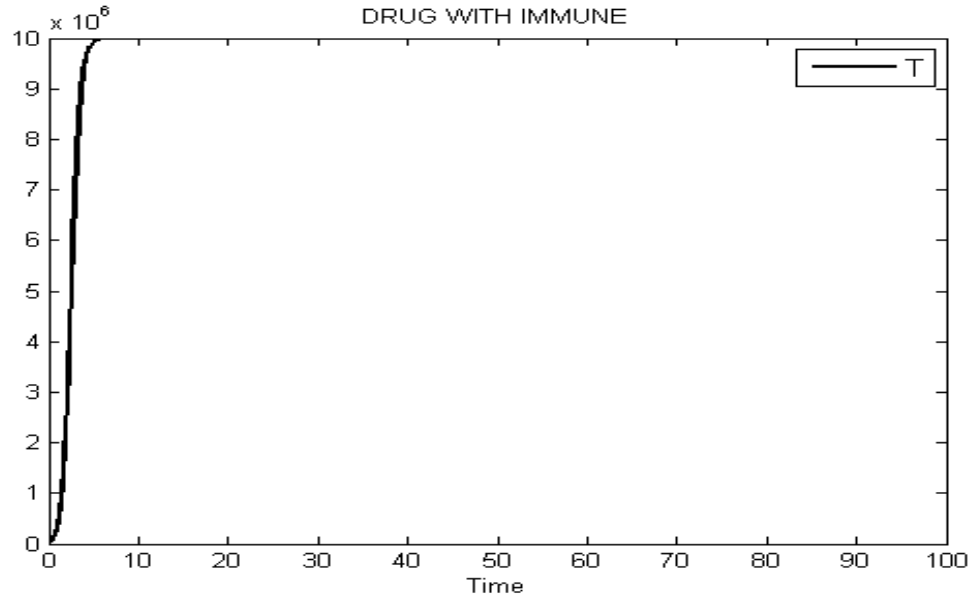

Figure 17a: Numerical solution curve for the uninfected cells in 100 days.

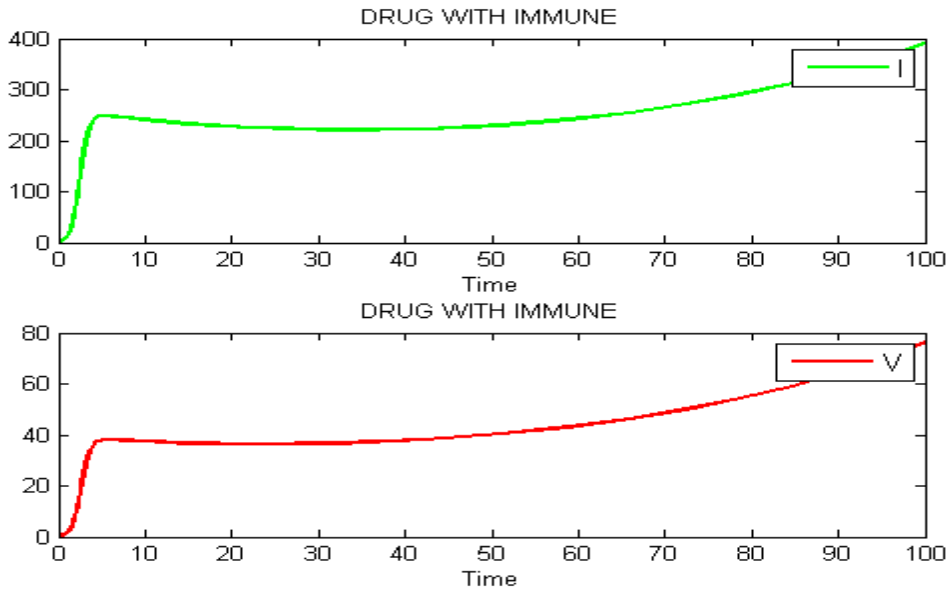

Figure 17b: Numerical solution curve for the infected cells and free virus in 100 days.

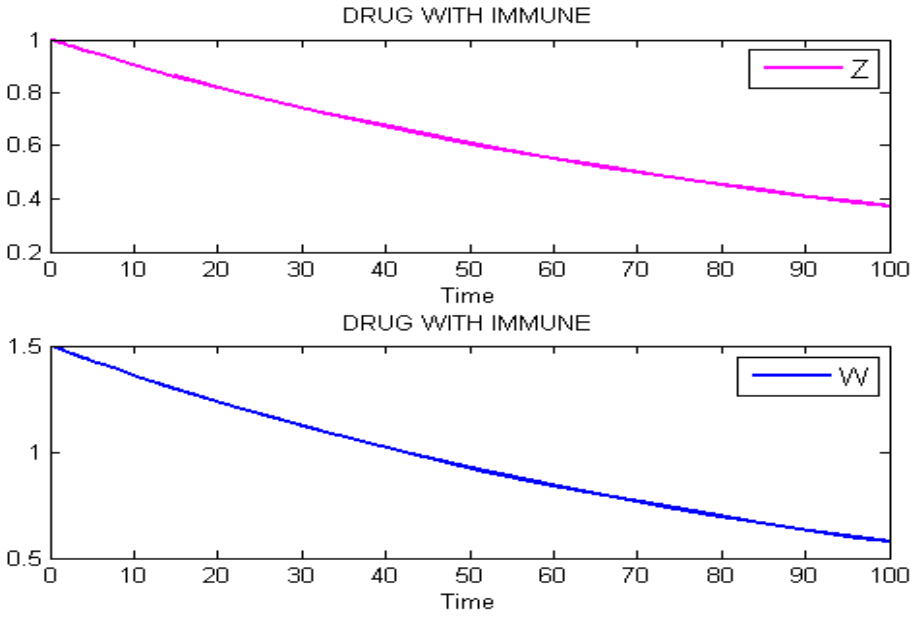

Figure 17c: Numerical solution curve for the CTLs and the antibody responses in 100 days.

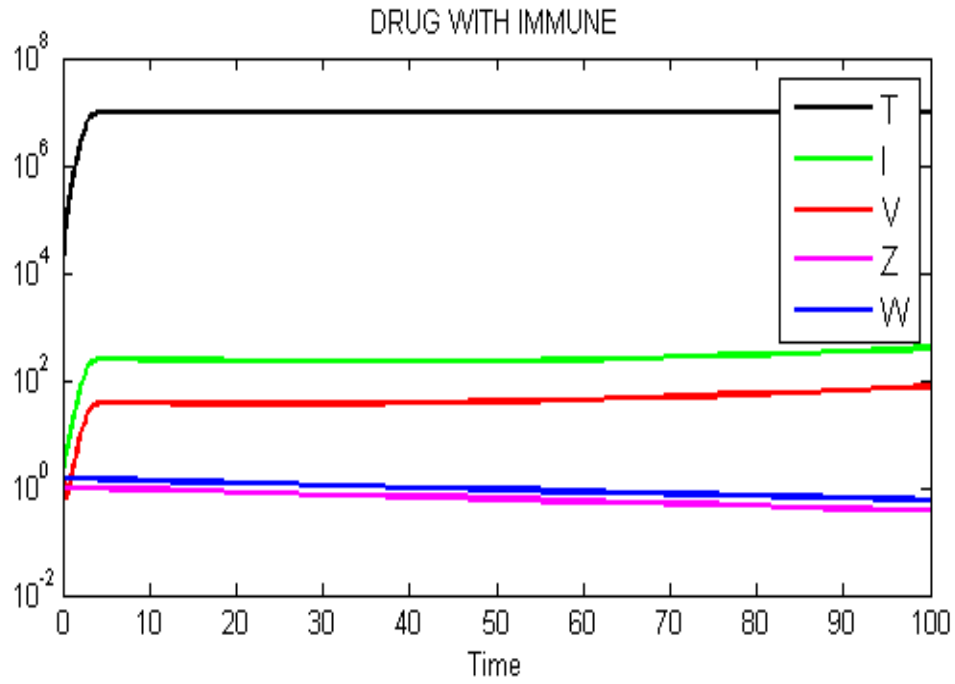

Figure 17d: Numerical simulation of the HCV model in 100 days.

4.11 Dominant CTL Responses Simulation

In this section, we want to illustrate the dominant CTL response. The value of parameters were chosen to illustrate this scenario from Table 2, but we change the parameters of p and q to $p = 8.4 * 10^{-4}$ and $q = 5.0*10^{-1}$. To indicate the case of a chronic infection, we chose large values for the initial conditions of the viral load and infected cells. Initial conditions: $T(0) = 1.0*10^{4}$; $I(0) = 2.0*10^{5}$; $V(0) = 3.0*10^{5}$; $Z(0) = 1.0*10^{0}$; $W(0) = 1.5*10^{0}$. The numerical simulation results are presented in Figure 18(a, b, c, d) and show that a strong proliferation of CTL leads to an extinction of the antibody response. In other word, the proliferation rate of CTLs is much stronger than the natural production rate of antibody.

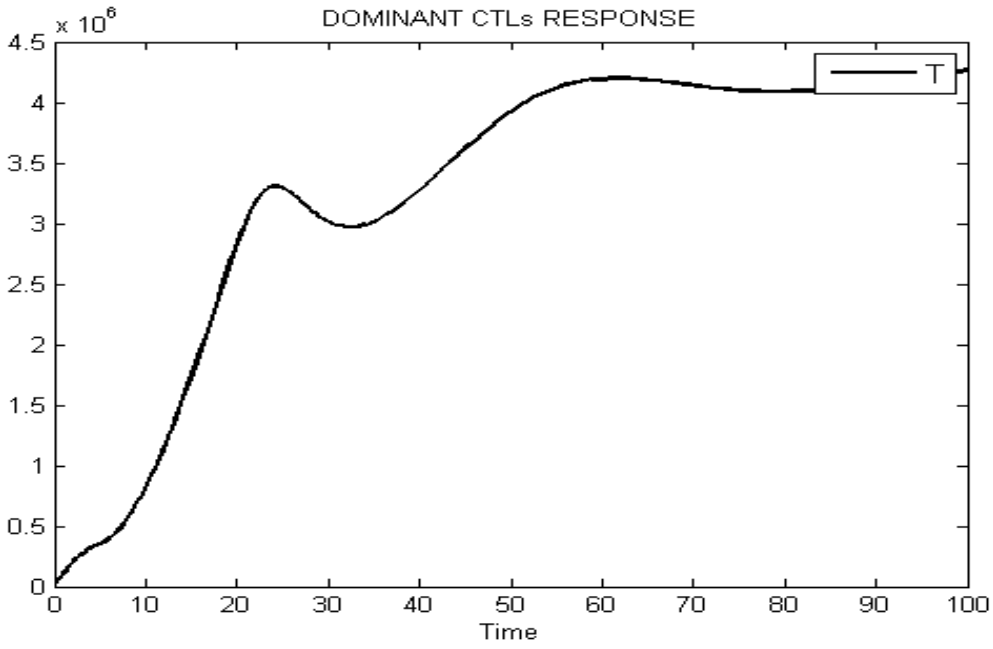

Figure 18a: Numerical solution curve for the uninfected cells in 100 days.

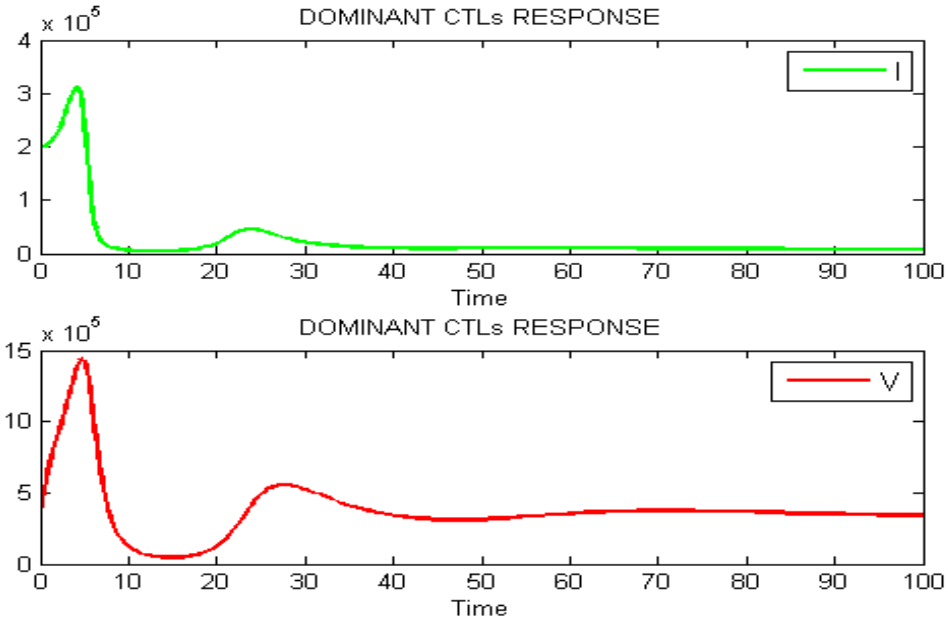

Figure 18b: Numerical solution curve for the infected cells and free virus in 100 days.

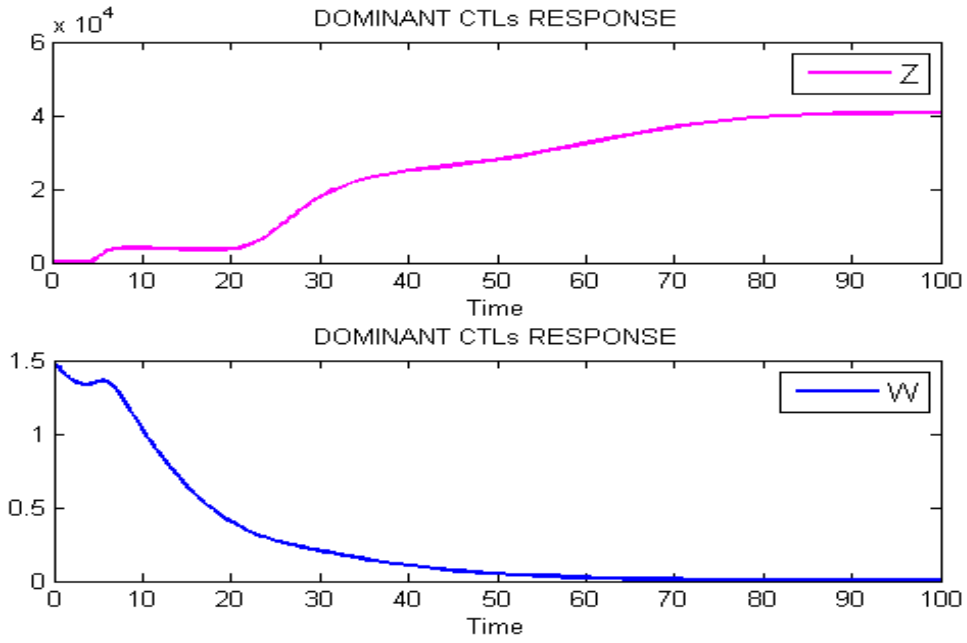

Figure 18c: Numerical solution curve for the CTLs and the antibody responses in 100 days.

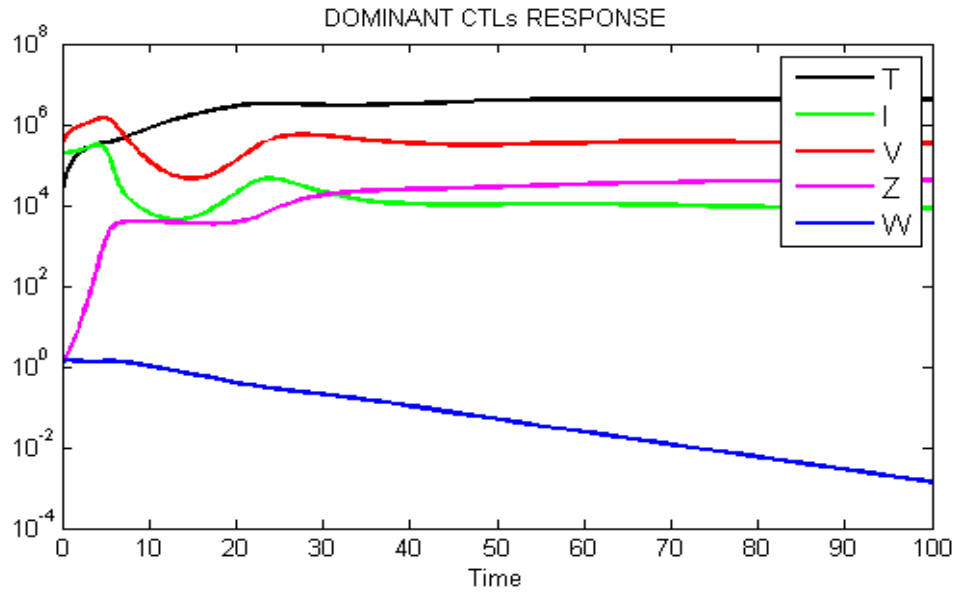

Figure 18d: Numerical simulation of the HCV model shows the dominant CTLs response in 100 days.

4.12 Dominant Antibody Response Simulation

In this section, we want to illustrate the dominant antibody response. The value of parameters were chosen to illustrate this scenario from Table 2, but we change the parameters of p and q to $p = 5.0 * 10^{-1}$ and $q = 8.4*10^{-4}$. To indicate the case of a chronic infection, we chose large values for the initial conditions of the viral load and infected cells. Initial conditions: $T(0) = 1.0*10^{4}$; $I(0) = 2.0*10^{5}$; $V(0) = 3.0*10^{5}$; $Z(0) = 1.0*10^{0}$; $W(0) = 1.5*10^{0}$. The numerical simulation results are presented in Figure 19(a, b, c, d) and show that a strong proliferation of antibody leads to an extinction of the CTL response. In other word, the proliferation rate of antibody is much stronger than the natural production rate of CTLs.

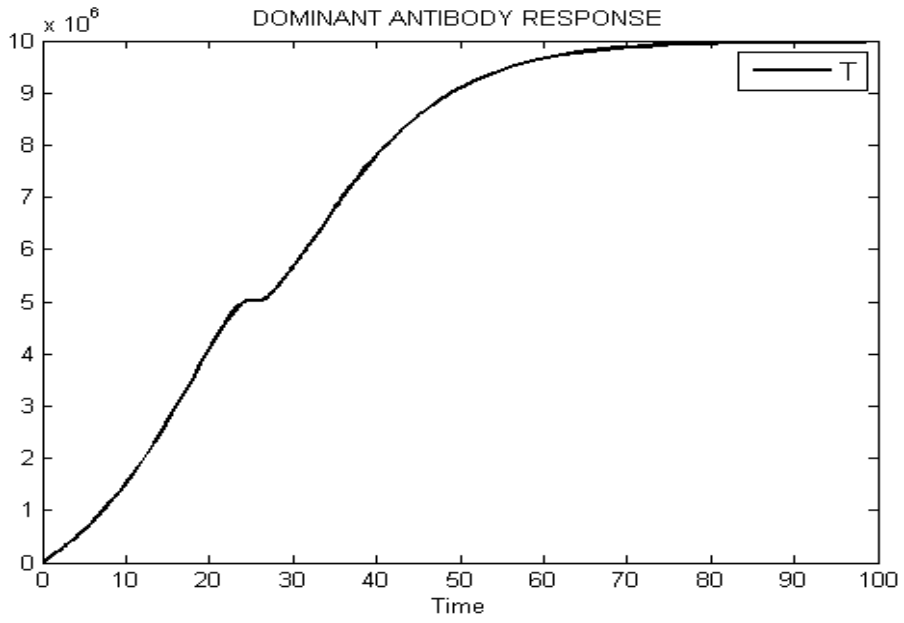

Figure 19a: Numerical solution curve for the uninfected cells in 100 days.

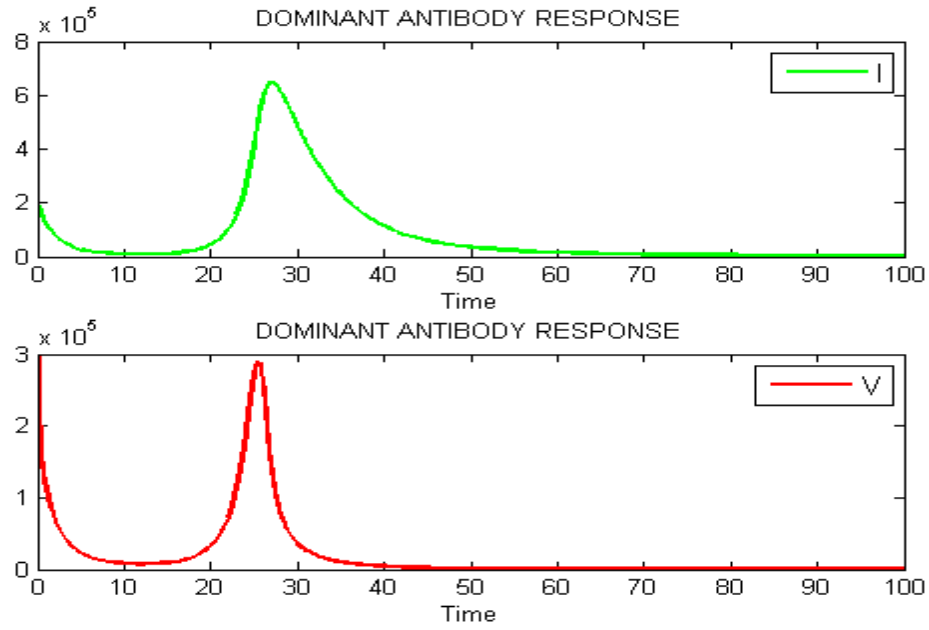

Figure 19b: Numerical solution curve for the infected cells and the free virus in 100 days.

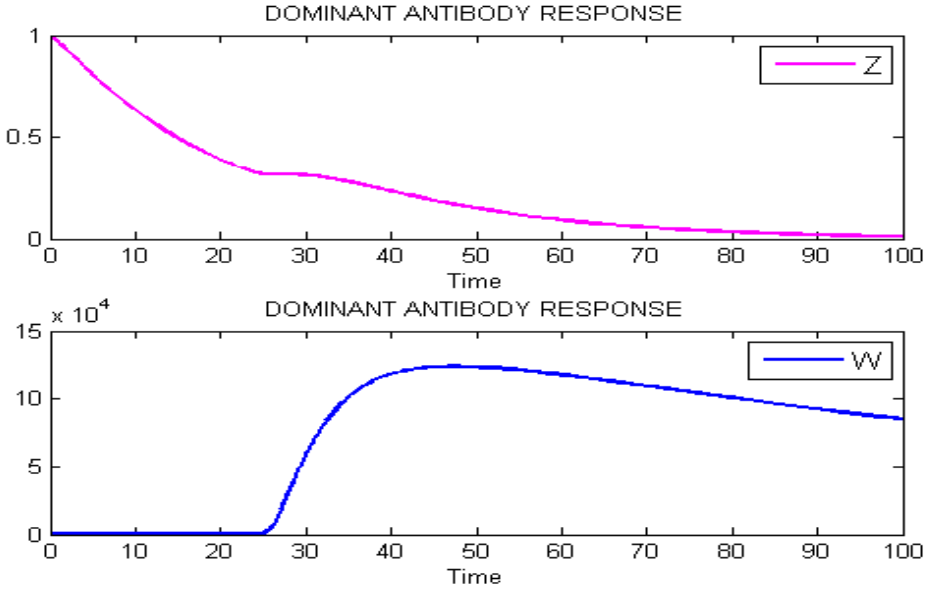

Figure 19c: Numerical solution curve for the CTLs and the antibody responses in 100 days.

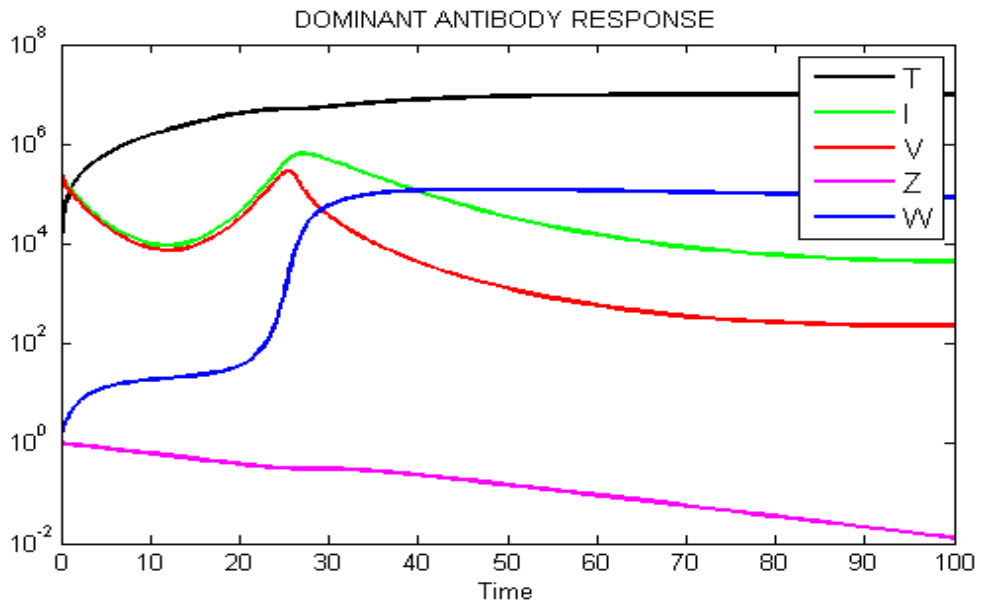

Figure 19d: Numerical simulation of the HCV model shows the dominant antibody response in 100 days.

4.13 Coexistence

In this section, we want to illustrate the CTL and antibody responses are equally recognized. The value of parameters were chosen to illustrate this scenario from Table 2, but we change the parameters of p and q to $p = 5.4* 10^{-4}$ and $q = 5.0*10^{-1}$. To indicate the case of a chronic infection, we chose large values for the initial conditions of the viral load and infected cells. Initial conditions*: $T(0) = 1.0*10^4$; $I(0) = 2.0*10^5$; $V(0) = 3.0*10^5$; $Z(0) = 1.0*10^0$; $W(0) = 1.5*10^0$.* The numerical simulation results are presented in Figure 20(a, b, c, d) and show that both CTL and antibody responses are equally determined. The two immune responses CTLs (T-cells) and antibody (B-cells) contend with each other to removal of the infection.

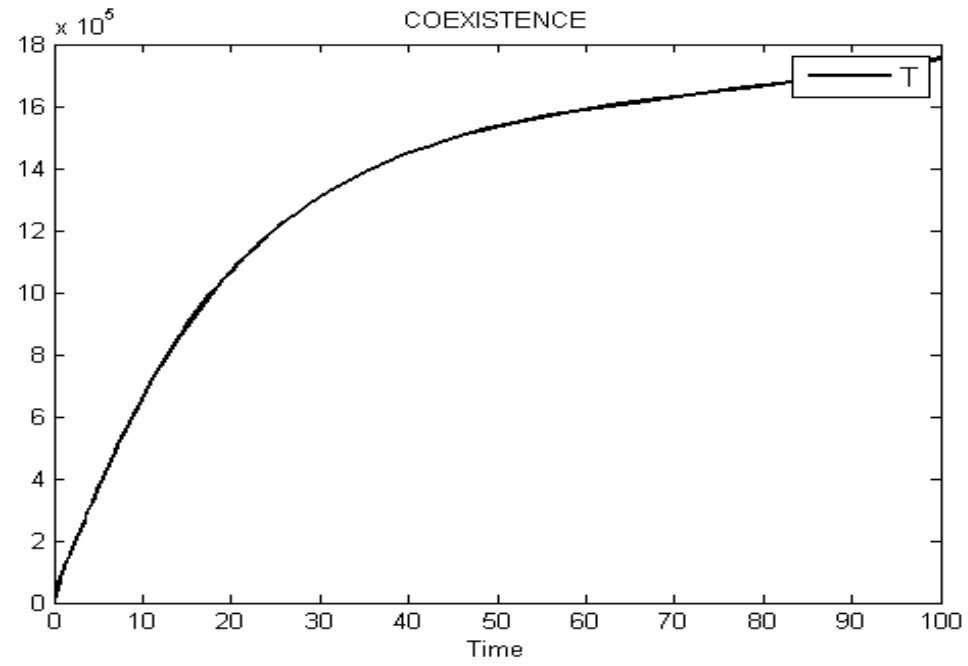

Figure 20a: Numerical solution curve for the uninfected cells in 100 days.

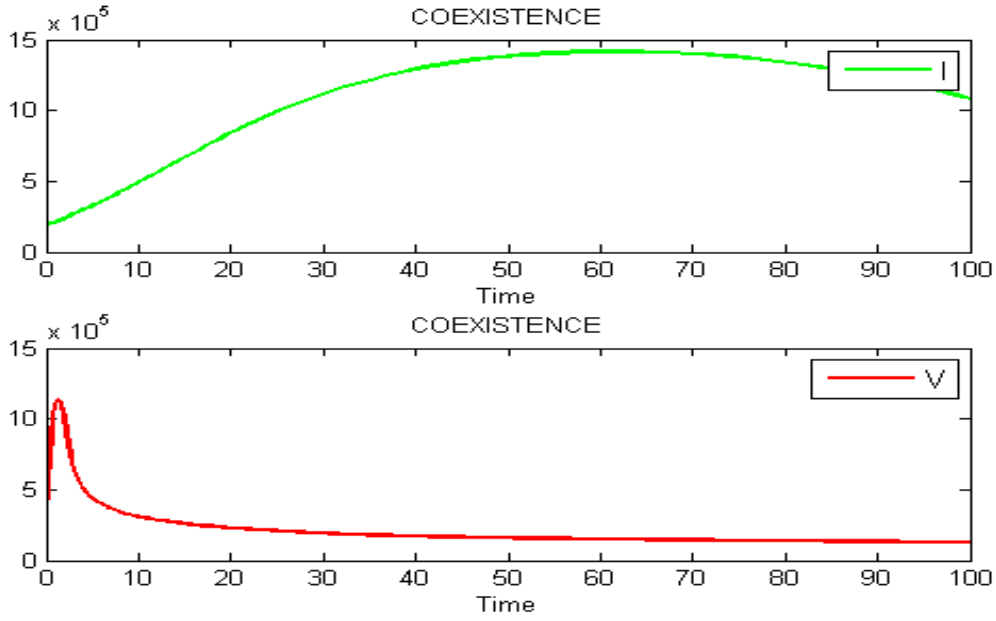

Figure 20b: Numerical solution curve for the infected cells and the free virus in 100 days.

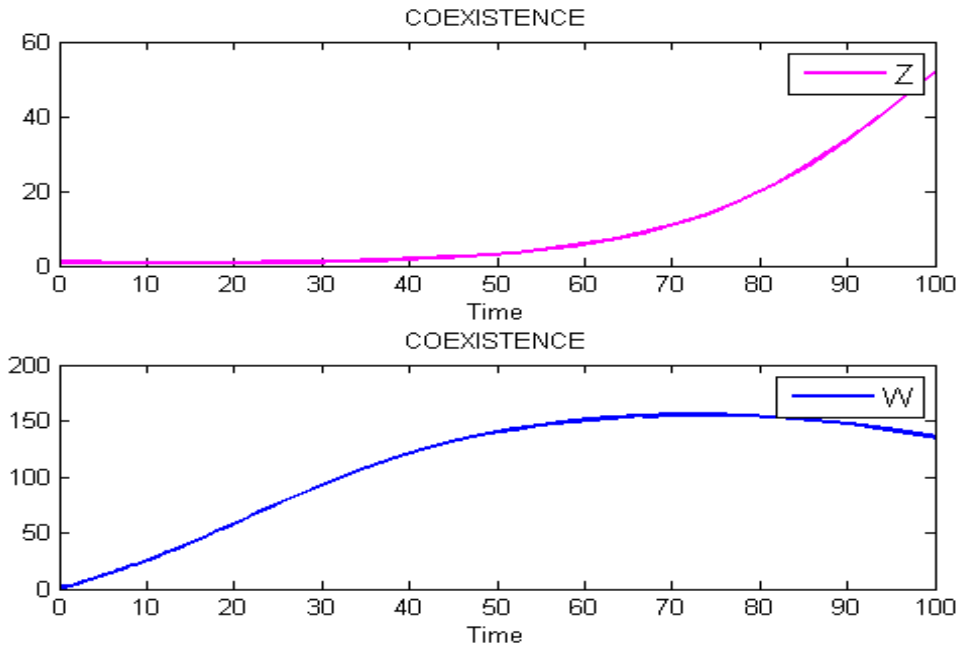

Figure 20c: Numerical solution curve for the CTLs and the antibody response in 100 days.

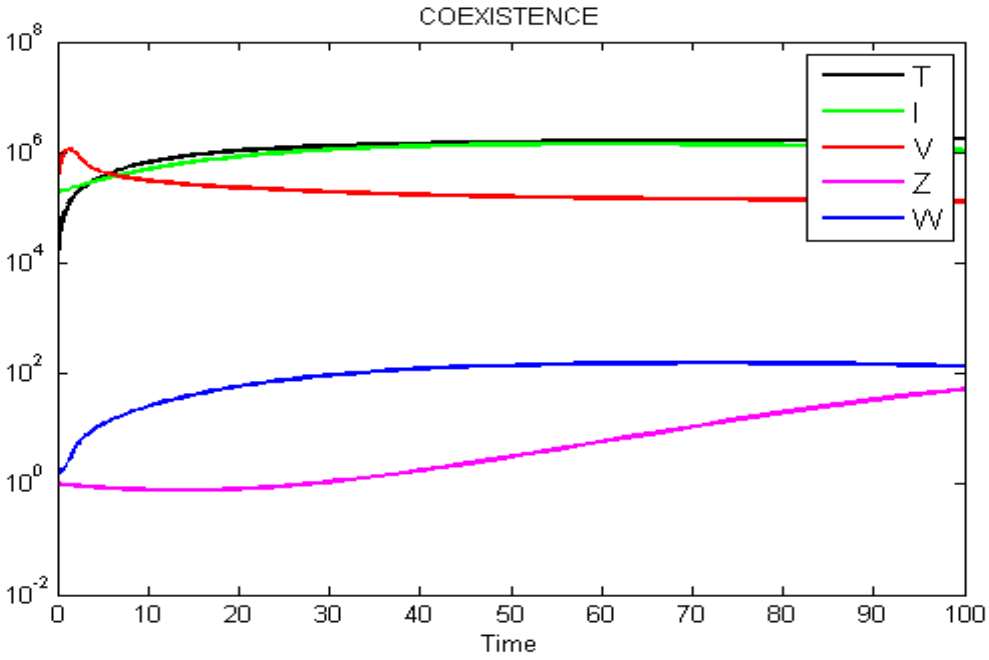

Figure 20d: Numerical simulation of the HCV model shows the Coexistence in 100 days.

5. CONCLUSSION

Hepatitis C is a dangerous disease caused by the hepatitis C infection (HCV) that essentially influences the liver. In this thesis, we have formulated a mathematical model (5) of ordinary differential equations for hepatitis C dynamic. This model is a combination of proliferation model (3) and immune responses model (4). Our model is considering the immune response to the HCV infection and accounts of the proliferation for the uninfected and infected hepatocytes. Also, it considers the mechanisms of cell death and killing by CTLs and antibody.

To determine the stability of the model, we evaluated the equilibrium points or steady states. In section 3.2.1, five equilibrium points of the model have been found explicitly. There are more equilibrium points that have been found by using Mathematica, but they are too complicated to write all of them in this thesis. The first equilibrium is called disease-free equilibrium which represents the absence of the virus. The next four equilibrium points are called the infected equilibria. The second equilibrium represents the absence of immune responses. Dominant CTLs response is represented by the third infected equilibrium. The fourth equilibrium represents the dominant antibody response. Coexistence is represented by the fifth infected equilibrium.

In section 3.2.2, we studied the stability properties of the disease-free equilibrium (uninfected steady state). The local stability of the disease-free equilibrium is ruled by five eigenvalues of the Jacobian matrix for this equilibrium. We found three eigenvalues directly, while the other two eigenvalues are solutions of the characteristic polynomial of a sub-Jacobian matrix of the system. Using the Routh-Hurwitz criteria, the two eigenvalues have negative real part since the coefficients of the characteristic polynomial are positive. This implies that the Routh-Hurwitz criteria condition is satisfied and the disease-free equilibrium is locally

asymptotically stable under this condition (3.2.2.2), which is found in section 3.2.2.1. Moreover, we found the values of the critical drug efficacy ε_c and η_c for successful drug therapy.

Next, we run simulations to verify the theoretical results in Chapter 3. Also, we showed the drug effectiveness and compared our model with other models. We predicted the behavior of the system under different drug effects, cells proliferation rate, and immune responses. We noticed that when drug and immune responses are zero, the disease-free equilibrium is unstable. Furthermore, when the drug effect is less than the critical drug efficacy, the disease-free equilibrium is again unstable. Also, if we increase the proliferation rate, the disease-free equilibrium is unstable.

Finally, we illustrated the dominant CTL response and the dominant antibody response. We changed the parameters of the neutralized rate of virus particles to be bigger than the killing rate of the infected cells. This showed that the proliferation rate of CTLs is much stronger than the natural production rate of antibody. Hence, the CTLs response increases and the antibody response become ineffective. Likewise, we changed the parameters of the neutralized rate of virus particles to be less than the killing rate of the infected cells. This showed the proliferation rate of antibody is stronger than the natural production rate of CTLs. Thus, the antibody response increases and the CTLs response become ineffective. Then, we made the parameters of the neutralized rate of virus particles and the killing rate of the infected cells to be equal. This showed that both CTL and antibody responses are equally determined. The two immune responses CTLs and antibody contend with each other to clearance of the infection.

The proposed model here represents HCV RNA decay under variety of treatment and takes into consideration both the immune system and cell proliferation. The study provides useful tools

not only for fitting HCV infections but also for modeling other similar infections with hepatocytes viruses, such as hepatitis A and B virus. This model allows predicting the viral decay and can help in understanding the kinetics of the HCV under different treatment. It can be used for better understanding the viral kinetics in patients.

References

[1] Allen, L., J., S., (2007). An Introduction to Mathematical Biology. *Department of Mathematics and Statistics Texas Tech University 2007 Pearson Education*. Inc. Upper Saddle River, NJ 07458.

[2] Alter, M., J., Margolis, H., S., Krawczynski, K., Judson, F., N., Mares, A., Alexander, WJ., Hu., P., Y., Miller, J., K., Gerber, M., A., and Sampliner, R., E. (1992). The natural history of community-acquired hepatitis C in the United States. *The Sentinel Counties Chronic non-A, non-B Hepatitis Study Team.* 327(27), 1899–1905. [PubMed: 1280771].

[3] Anderson, R., M., and May, R. (1991). Infectious diseases of humans: dynamics and control. *Oxford: Oxford University Press*.

[4] Brauer, F. (2004). The analysis of some characteristic equations rising in population and epidemic models. *Journal of Dynamics and Differential Equations*, 16, 441-453. http://dx.doi.org/10.1007/s10884-004-4287-z

[5] Callaway, D., S., and Perelson, A., S. (2002). HIV-1 infection and low steady state viral loads. *Bull Math Biol*, 64(1), 29–64. doi: 10.1006/bulm.2001.0266

[6] Chaplin, D., D. (2010). Overview of the Immune Response. *The Journal of allergy and clinical immunology*, 125(2), Suppl 2, S3–S23. doi: 10.1016/j.jaci.2009.12.980

[7] Choo, Q., L., Kuo, G., Weiner, A., J., Overby, L., R., Bradley, D., W., and Houghton, M. (1989, April 21). Isolation of a cDNA clone derived from a blood-borne non-A, non-B viral hepatitis genome. *Science (New York, N.Y.)* 244(4902), 359–363.

[8] Dahari, H., Loa, A., Ribeiroa, R. M., and Perelson, A. S. (2007, July 21). Modeling hepatitis C virus dynamics: Liver regeneration and critical drug efficacy. *Journal of Theoretical Biology*, 247(2), 371–381. https://doi.org/10.1016/j.jtbi.2007.03.006

[9] Davis, C., P., and Marks, J., W. (2017). Hepatitis (viral Hepatitis, A, B, C, D, E, G). http://www.medicinenet.com/viral_hepatitis/article.htm

[10] Davis, G., L., Albright, J., E., Cook, S., F., and Rosenberg, D., M. (2003). Projecting Future Complications of Chronic Hepatitis C in the United States. *Liver Transplantation*, 9(4), 331-338. doi:10.1053/jlts.2003.50073

[11] Delves, P., J. and Roitt, I., M. (2000, July 6). Advances in Immunology. *The New England Journal of Medicine*, 343(1), 37-49. doi: 10.1056/NEJM200007063430107

[12] De Oliveria Andrade, L. J., D'Oliveira, A., Melo, R. C., De Souza, E. C., Costa Silva, C. A., & Paraná, R. (2009). Association Between Hepatitis C and Hepatocellular Carcinoma. *Journal of Global Infectious Diseases*, *1*(1), 33–37. http://doi.org/10.4103/0974-777X.52979

[13] Driessche, P., V., D., and Watmough, J. (2002). Reproduction numbers and sub-threshold endemic equilibria for compartmental models of disease transmission. *Mathematical Biosciences*, 180, 29–48.

[14] Farci, P., Shimoda, A., Coiana, A., Diaz, G., Peddis, G., Melpolder, J., C., … Alter, H., J. (2000). The outcome of acute hepatitis C predicted by the evolution of the viral quasispecies. *Science*, 288(5464), 339–344.

[15] Fausto, N. (2004). Liver regeneration and repair: Hepatocytes, progenitor cells, and stem cells. *Hepatology*, 39 (6), 1477–1487.

[16] Gremion, C., and Cerny, A. (2005, March 22). Hepatitis C Virus and the Immmune System: a Concise Review. *Reviews in Medical Virology*. 15. 4: 235–268. doi:10.1002/rmv.466

[17] Guedj, J., Dahari, H., Rong, L., Sansone, N., D., Nettles, R., E., Cotler, S., J., Layden, T., J., Uprichard, S., L., Perelson, A., S. (2013, March 5). Modeling shows that the Ns5A inhibitor Daclatasvir has two modes of action and yields a shorter estimate of the hepatitis c virus half-life. *PNAS*. 110(10), 3991-6. doi: 10.1073/pnas.1203110110

[18] Hoofnagle, J., H. (2002). Course and Outcome of Hepatitis C. *Hepatology*. 36(5):S21–29. https://doi.org/10. 1053/jhep.2002.36227 PMID: 12407573

[19] How does the liver work? August 22, 2016. https://www.ncbi.nlm.nih.gov/pubmedhealth/PMH0072577/

[20] Janeway, C., A., Jr, Travers, P., Walport, M., and Shlomchik, M., J. (2001). Immunobiology: The Immune System in Health and Disease. 5th edition. New York: Garland Science. Available from: https://www.ncbi.nlm.nih.gov/books/NBK27090/

[21] Jirillo, E. (2008). *Hepatitis C virus Disease: Immunobiology and Clinical Applications*, Springer.

[22] Jones, J., H. (2007). Notes On R_0. *Department of Anthropological Sciences*. Stanford University.

[23] Klenerman, P., Lechner, F., Kantzanou, M., Ciurea, A., Hengartner, H., and Zinkernagel, R. (2000). Viral escape and the failure of cellular immune responses. *Science*, 289(5487), 2003. doi: 10.1126/science.289.5487.2003a

[24] Kohli, A., Shaffer, A., Sherman, A., Kottilil, S.(2014). Treatment of Hepatitis CA Systematic Review. *JAMA*, 312(6), 631-640. doi:10.1001/jama.2014.7085

[25] Leenheer, P., D., and Smith, H., L. (2003). VIRUS DYNAMICS: A GLOBAL ANALYSIS. *SIAM J. APPL. MATH*, 63(4), 1313–1327.

[26] Libin, R., Harel, D., Ruy, M., R., and Alan, S., P. (2010, May 5). Rapid Emergence of Protease Inhibitor Resistance in Hepatitis C Virus. *Science Translational Medicine*, 2(30), 30-32. doi: 10.1126/scitranslmed.3000544

[27] Medzhitov, R., and Janeway, C., Jr. (2000, August 2). Innate immunity. *N. Engl. J. Med*, 343(5), 338–344. doi: 10.1056/NEJM200008033430506

[28] Michalopoulos, G., K., and DeFrances, M., C. (1997). Liver Regeneration. *Science*, 276 (5309), 60–66.

[29] Neumann, A., U., Lam, N., P., Dahari, H., Gretch, D., R., Wiley, T., E., Layden, T., J., and Perelson, A., S. (1998). Hepatitis C viral dynamics in vivo and the antiviral efficacy of interferon-alpha therapy. *Science*, 282(5386), 103–107.

[30] Nguyen, T., and Guedj, J. (2015). HCV Kinetic Models and Their Implications in Drug Development. *CPT: Pharmacometrics & Systems Pharmacology*, 4(4), 231–242. http://doi.org/10.1002/psp4.28

[31] Nowak, M., A., and Bangham C., R., M. (1996, April 5). Population Dynamics of Immune Responses to Persistent Viruses, *Science*, New Series, 272 (5258), 74-79.

[32] Nowak, M., A., and May, R., M. (2000). Virus Dynamics: Mathematical Principles of Immunology and Virology. *Oxford University Press*.

[33] Payne, R., J., H., Nowak, M., A., and Blumberg, B., S. (1996). The dynamics of hepatitis B virus infection, *Proc. Natl. Acad. Sci*. USA, 93, 6542-6546.

[34] Perelson, A., S., Herrmann, E., Micol, F., Zeuzem, S. (2005). New kinetic models for the hepatitis C virus. *Hepatology*, 42(4),749–754. [PubMed: 16175615].

[35] Perelson, A., S., Neumann, A., U., Markowitz, M., Leonard, J., M., and Ho, D., D. (1996, March 15). HIV-1 dynamics in vivo: virion clearance rate, infected cell life-span, and viral generation time. *Science*, 271 (5255), 1582-1586.

[36] Ramirez, I. (2014). Mathematical Modeling of Immune Responses to Hepatitis C Virus Infection. *Electronic Theses and Dissertations*. Paper 2425. http://dc.etsu.edu/etd/2425

[37] Rong, J., Guedj, J., Dahari, H., Coffield, D., J., Levi, M., Smith, P., and Perelson, A., L. (2013, March 14). Analysis of Hepatitis C Virus Decline during Treatment with the Protease Inhibitor Danoprevir Using a Multiscale Model. *PLOS Comput Biol* 9(3): e1002959. https://doi.org/10.1371/journal.pcbi.1002959

[38] Shudo, E., Ribeiro, R. M., and Perelson, A. S. (2009). Modeling Hepatitis C Virus Kinetics under Therapy using Pharmacokinetic and Pharmacodynamic Information. *Expert Opinion on Drug Metabolism & Toxicology*, 5(3), 321–332. http://doi.org/10.1517/17425250902787616

[39] Viral Hepatitis. *U.S. Department of Health and Human Services, Office on Women's Health*. July 1, 2010. https://www.womenshealth.gov/files/assets/docs/fact-sheets/viral-hepatitis.pdf

[40] Wein L, D., R., and Perelson, A. (1998). Mathematical analysis of antiretroviral therapy aimed at HIV-1 eradication or maintenance of low viral loads. *Journal of Theoretical Biology*, 192, 81-98. PubMed ID: 9628841.

[41] Wodarz, D. (2003). Hepatitis C virus dynamics and pathology: the role of CTL and antibody responses. *Journal of General Virology*, 84, 1743-1750.

[42] Wodarz, D. (2007). Killer Cell Dynamics: Mathematical and Computational Approaches to Immunology, *Interdisciplinary Applied Mathematics*. Springer New York.

[43] World Health Organization (2014, April). Hepatitis C. Fact sheet no.164.

[44] Yousfi, N., Hattaf, K., and Rachik, M. (2009). Analysis of a HCV Model with CTL and Antibody Responses . *Applied Mathematical Sciences*, 3 (57), 2835-2846.

[45] Zeuzem, S., Schimdt, J., M., Lee, J., H., Ruster, B., and Roth, W., K. (1996). Effect of Interferon Alpha on the dynamics of Hepatitis C virus turnover in vivo. *Hepatology*, 23 (2), 366 – 371.

[46] Zeuzem, S., Schimdt, J., M., Lee, J., H., Von-Wagner, M., Teuber, G., and Roth, W., K. (1998). Hepatitis C virus dynamics in vivo: effect of ribavirin and interferon alpha on viral turnover. *Hepatology*, 28 (1), 245 – 252.